Human Molecular Genetics, 2012, Vol. 21, No. 13 **2973–2990**
doi:10.1093/hmg/dds128
Advance Access published on April 5, 2012

Mitochondria-targeted catalase reduces abnormal APP processing, amyloid β production and BACE1 in a mouse model of Alzheimer's disease: implications for neuroprotection and lifespan extension

Peizhong Mao[1], Maria Manczak[1], Marcus J. Calkins[1], Quang Truong[1], Tejaswini P. Reddy[1], Arubala P. Reddy[1], Ulziibat Shirendeb[1], Herng-Hsiang Lo[2], Peter S. Rabinovitch[3] and P. Hemachandra Reddy[1,4,*]

[1]Division of Neuroscience, Oregon National Primate Research Center, Oregon Health & Science University, 505 NW 185th Avenue, Beaverton, OR 97006, USA, [2]The University of Texas at Austin College of Pharmacy, Austin, TX 78712, USA, [3]Department of Pathology, University of Washington, 1959 Pacific Ave NE, HSB-K081, Seattle, WA 98195, USA and [4]Department of Physiology and Pharmacology, Oregon Health & Science University, 3181 SW Sam Jackson Park Road, Portland, OR 97239, USA

Received March 4, 2012; Revised March 23, 2012; Accepted April 2, 2012

The purpose of this study was to investigate the protective effects of the mitochondria-targeted antioxidant catalase (MCAT) and lifespan extension in mice that express amyloid beta (Aβ). Using immunoblotting and immunostaining analyses, we measured the production of full-length amyloid precursor protein (APP), soluble APPα, C-terminal fragments CTF99 and CTF83, monomeric and oligomeric Aβ, Aβ deposits and beta site amyloid precursor protein cleaving enzyme 1 (BACE1), in different stages of disease progression in MCAT/AβPP and AβPP mice. Using quantitative reverse transcriptase polymerase chain reaction and immunostaining analyses, we studied the expression of catalase, BACE1, the Alzheimer's disease (AD) markers, synaptophysin, APP, neprilysin, insulin-degrading enzyme and transthyretin in MCAT, AβPP, MCAT/AβPP and wild-type (WT) mice. Using the high pressure liquid chromatography analysis of 8-hydroxy-2-deoxyguanosine, we measured oxidative DNA damage in the cerebral cortical tissues from MCAT, AβPP, MCAT/AβPP and WT mice. We found that the AβPP transgenic mice that carried the human MCAT gene lived 5 months longer than did the AβPP mice. We also found that the overexpression of MCAT in the brain sections from the MCAT/AβPP transgenic mice significantly correlated with a reduction in the levels of full-length APP, CTF99, BACE1, Aβ levels (40 and 42), Aβ deposits and oxidative DNA damage relative to the brain sections from the AβPP mice. Interestingly, we found significantly increased levels of soluble APPα and CTF83 in the MCAT/AβPP mice, relative to the AβPP mice. These data provide direct evidence that oxidative stress plays a primary role in AD etiopathology and that in MCAT mice express Aβ, MCAT prevents abnormal APP processing, reduces Aβ levels and enhances Aβ-degrading enzymes in mice at different ages, corresponding to different stages of disease progression. These findings indicate that mitochondria-targeted molecules may be an effective therapeutic approach to treat patients with AD.

*To whom correspondence should be addressed at: Neurogenetics Laboratory, Division of Neuroscience, Oregon National Primate Research Center, West Campus, Oregon Health & Science University, 505 NW 185th Avenue, Beaverton, OR 97006, USA. Tel: +1-5034182625; Fax: +1-5034182701; Email: reddyh@ohsu.edu

INTRODUCTION

Alzheimer's disease (AD) is the most common neurodegenerative disorder and is characterized by learning and memory deficits and the progressive accumulation of amyloid beta (Aβ) in the brain regions of learning and memory (1–4). It is generally accepted that Aβ accumulation in the brain leads to a cascade of cellular changes in AD pathogenesis, and its reduction or clearance from the brain may be an important therapeutic strategy for prevention and treatment of AD. The most common Aβ peptides are Aβ40 and Aβ42. In early onset familial AD, genetic mutations in the AβPP gene were found to enhance Aβ40 and Aβ42 levels and mutations in the presenilin 1 and 2 genes were found to enhance Aβ42 levels (5). However, in late-onset AD, the increased production of reactive oxygen species (ROS) has been hypothesized to increase β- and γ-secretases and to produce Aβ (6). Several papers have provided data to support this hypothesis (7–9). Oxidative stress was found to produce Aβ pathology in AD progression (10,11). Aβ pathology was found to further increase ROS levels and increased ROS levels in turn produced more Aβ, ultimately damaging the structure and functioning of mitochondria (12).

In studies of Aβ and mitochondria, AD postmortem brains (13–17), AD cells (16–21), AD transgenic mouse models (19–25) and gene expression studies (13,20,26), mitochondrial dysfunction was found to be involved in early AD progression. However, the precise connection between Aβ and mitochondrial dysfunction was unclear until recently. Recent evidence from our lab (19,21,26) and others (14,15,22,24,25,27–29) found that Aβ is localized to mitochondria, induces free radical production, decreases cytochrome oxidase, inhibits mitochondrial ATP, impairs mitochondrial dynamics, interferes with the axonal transport of mitochondria and damages neuronal function in AD neurons. However, the protective effects of mitochondria-targeted antioxidants against Aβ-induced mitochondrial damage from birth to death have not been determined.

Scavenging free radicals and decreasing oxidative stress and mitochondrial dysfunction in AD neurons have been hypothesized to decrease neuronal damage and extend neuronal survival. The ideal approach to investigate this possibility is to enhance endogenous antioxidant levels or to introduce exogenously antioxidants targeted to mitochondria. To determine the role of mitochondria-targeted antioxidant, catalase in scavenging free radicals and extending the lifespan in mice, Schriner *et al*. (30) created transgenic mouse lines that overexpress human catalase that is localized to peroxisomes (PCAT mice), nuclei (NCAT mice) and mitochondria [mitochondria-targeted antioxidant catalase (MCAT) mice]. The MCAT transgenic mice showed about a 20% increase in median and maximal lifespan compared with the lifespan of non-transgenic, age-matched, wild-type (WT) littermates (30). However, the impact of catalase targeted to mitochondria, particularly in the brain, has not yet been determined.

In the studies reported here, we sought to determine the protective effects of MCAT against abnormal amyloid precursor protein (APP) processing, Aβ pathology and lifespan extension, if any, using the MCAT (30) and AβPP (Tg2576 line) (31) mouse lines. First, we crossed MCAT mice with AβPP mice to study the resultant double-transgenic mouse line MCAT/AβPP. We compared neurons from the MCAT/AβPP mice with the MCAT, AβPP and non-transgenic WT mice in terms of: (i) lifespan and mortality, (ii) abnormal APP processing events, including the production of full-length APP, C-terminal fragments CTF99 and CTF83 and soluble APPα, (iii) Aβ production (40 and 42 levels), Aβ deposits, Aβ oligomers, beta site amyloid precursor protein cleaving enzyme 1 (BACE1) expression and its activity, (iv) oxidative DNA damage and (v) the AD markers, synaptophysin, APP, neprilysin, insulin-degrading enzyme and transthyretin (TTR). We studied the mice at three ages correspond to three stages of disease progression: 6, 12 and 24 months.

RESULTS

Generation of MCAT/AβPP mice

To investigate the protective effects of overexpressed human catalase in AD progression and pathogenesis, we crossed MCAT mice with AβPP mice and developed the double-mutant mouse line MCAT/AβPP. Littermates of four different genotypes were produced: MCAT, AβPP, MCAT/AβPP and non-transgenic WT mice (controls). We genotyped and identified them with the PCR analysis of tail and/or ear DNA.

Lifespan and mortality in the transgenic and WT mice

To determine whether the expression of MCAT modulates the healthy lifespan of the MCAT/AβPP mice and WT mice, we combined data from both genders of these mice. Figure 1 gives those data. MCAT mice had an extended median lifespan was 5 months longer compared with the WT mice ($P < 0.001$, Fig. 1A), and a maximum lifespan was 5 months longer than their non-transgenic counterparts.

We next compared the lifespan of AβPP and WT littermates. The median lifespan of the AβPP mice was shorter by 6 months ($P < 0.001$, Fig. 1C) and the maximum lifespan shorter by 3.5 months. In a comparison of the median and maximum lifespans of the MCAT and AβPP mice, the MCAT median lifespan was longer by 6 months ($P < 0.001$, Fig. 1D) and the maximum lifespan was longer by 7 months. We also sought to determine whether MCAT/AβPP mice had lower levels of Aβ and whether these levels extended the lifespan of these mice. The median lifespan of the MCAT/AβPP mice was longer by 4 months, compared with their AβPP littermates ($P < 0.05$, Fig. 1B), and the maximum lifespan of the MCAT/AβPP mice was also longer by 5 months. Our preliminary analysis of gender-based lifespan in WT and MCAT mice revealed that 65% MCAT female mice live beyond 20 months and 50% MCAT male mice live beyond 20 months, indicating that MCAT protect female mice better than male mice.

We then determined conditions of the mice at the time of death. As shown in Table 1, in the WT mice, 26.87% (15 of 56) had tumors, 8% (10 of 56) were dehydrated and had prolapses, 14% (8 of 56) had skin problems and 7% (4 of 56) had respiratory problems. Multiple conditions affected the AβPP mice. As shown in Table 1, 23% (6 of 26) had tumors, 5.3% (4 of 26) were small and died prematurely, 11.5% had

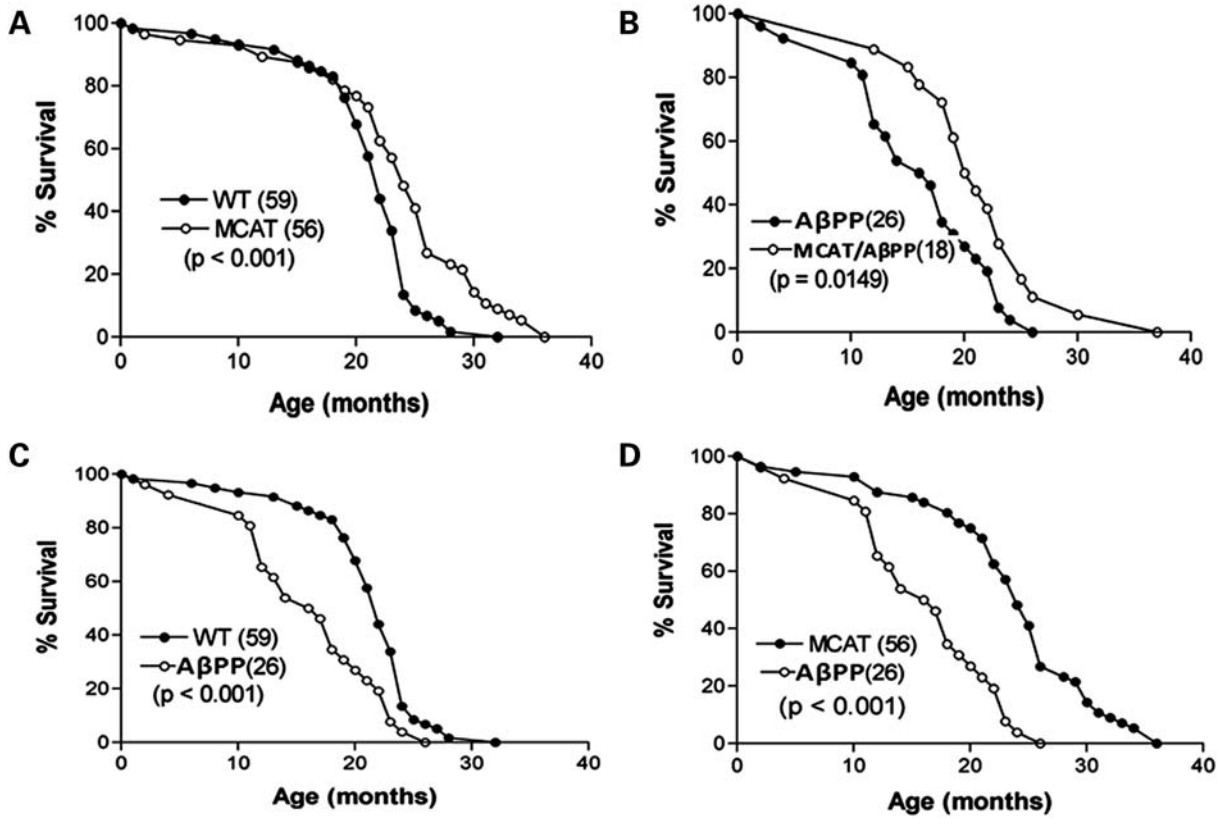

Figure 1. Lifespan analysis of transgenic and WT mice. Survival was analyzed for: (**A**) MCAT and WT, (**B**) AβPP and MCAT/AβPP, (**C**) AβPP and WT and (**D**) MCAT and AβPP. The number of mice in each genotype is shown in parentheses following the genotype. *P*-values of significant differences in mean lifespan between genotypes are also indicated.

Table 1. Health factors found in autopsy of WT mice and lines transgenic littermates (birth to death)

Health factors found in autopsy	WT		AβPP		MCAT		MCAT/AβPP	
	n	Percentage	*n*	Percentage	*n*	Percentage	*n*	Percentage
Tumors	15	26.8	6	23.1	12	24.0	3	16.7
Skin problems	8	14.2	2	7.7	6	12.0	1	5.5
Dehydrated, prolapsus	10	17.9	2	7.7	7	14.0	5	27.8
Hydrocephalus	0	0.0	3	11.5	0.0	0.0	0.0	0.0
Eye infection, problems and paralysis	0	0.0	2	7.7	0.0	0.0	1	5.5
Premature death	0	0.0	4	15.3	0.0		0.0	0.0
Respiratory problems	4	7.1	2	7.7	9	18.0	2	11.1
Unknown factors	19	34.0	5	19.2	16	32	6	33.3
Total	56		26		50		18	

hydrocephalus and 7.7% each had skin problems, hydration/prolapses, eye problems and respiratory problems. Also as shown in Table 1, multiple conditions were present at the deaths of the MCAT and the MCAT/AβPP mice, but they did not exhibit hydrocephalus and none expired prematurely.

Effect of MCAT on mRNA expressions

We determined the role of MCAT in protecting the MCAT/AβPP, MCAT and AβPP mice and the WT littermates at 6, 12 and 24 months of age (Table 2), and we compared the AβPP mouse data with the data from the MCAT/AβPP mice (Table 3). We used quantitative real-time RT–PCR with Sybr-Green chemistry and quantified the mRNA in several genes critical for AD progression. These genes included APP, NEP, BACE1, IDE, TTR and synaptophysin.

We found catalase levels higher in the 6- (1.2-fold), 12- (3.5-fold, $P < 0.005$) and 24-month-old (1.3-fold) MCAT mice, relative to the WT mice (Table 2), and catalase levels were significantly lower than those of WT mice, in the 6- (-2.7-fold, $P < 0.05$) and 24-month-old (-2.0-fold, $P < 0.05$) AβPP mice. Catalase levels in the 6- (2.2-fold, $P < 0.05$), 12- (2.9-fold, $P < 0.05$) and 24-month-old (1.9-fold, $P < 0.05$) MCAT/AβPP mice were significantly higher compared with those in the WT mice (Table 2). As shown in Table 3, catalase levels were also significantly higher in

Table 2. mRNA fold changes of genes related to Aβ in 6-, 12- and 24-month-old MCAT, AβPP and MCAT/AβPP mice, relative to WT mice

	6 months			12 months			24 months		
	MCAT	AβPP	MCAT/AβPP	MCAT	AβPP	MCAT/AβPP	MCAT	AβPP	MCAT/AβPP
Catalase	1.2	−2.7*	2.2*	3.5**	1.3	2.9*	1.3	−2.0*	1.9*
Synaptophysin	1.5	−3.7*	1.8*	2.2**	−1.4*	2.7**	3.7**	1.7	2.4*
BACE1	1.3	1.8*	1.5	−3.6**	3.3**	1.4	−1.4	2.2*	1.2
APP	−1.2	1.7	1.2	−1.6	1.61	−2.3*	−1.4	1.8*	−1.5
Neprilysin	2.6*	−1.2	2.5*	1.5	−1.4*	1.2	1.3	−1.3*	1.5*
Insulin-degrading enzyme	3.5*	−2.7*	−1.6	2.1*	−1.9*	1.9*	1.8*	−1.5*	1.9**
TTR	1.5	−1.4*	2.6*	1.1	−1.2	2.1*	1.3	−1.8*	1.9*

*$P \leq 0.05$.
**$P \leq 0.005$.

the 6- (5.4-fold, $P < 0.005$), 12- (2.0-fold, $P < 0.05$) and 24-month-old (2.1-fold, $P < 0.05$) MCAT/AβPP mice, relative to the AβPP mice.

As expected, the mRNA expression of synaptophysin decreased in the 6- (−3.7-fold, $P < 0.05$) and 12-month-old (−1.4-fold, $P < 0.05$) AβPP mice, compared with the WT mice, indicating a progressive loss of synaptophysin as the AβPP mice aged. In contrast, synaptophysin levels were significantly increased in the MCAT/AβPP mice, relative to the WT mice (Table 2). In the MCAT mice, synaptophysin levels were significantly higher in the 12- (2.2-fold, $P < 0.005$) and 24-month-old (3.7-fold, $P < 0.005$) mice, relative to the levels in the WT mice (Table 2). As shown in Table 3, synaptophysin levels were significantly higher in the 6- (5.3-fold, $P < 0.005$), 12- (2.3-fold, $P < 0.05$) and 24-month-old (4.3-fold, $P < 0.005$) MCAT/AβPP mice, relative to the AβPP mice. These findings indicate that catalase, when targeted to mitochondria, enhances synaptophysin in MCAT and MCAT/AβPP mice.

BACE1 mRNA expressions were significantly higher in the 6- (1.8-fold, $P < 0.05$), 12- (3.3-fold, $P < 0.005$) and 24-month-old (2.2-fold, $P < 0.05$) AβPP mice, relative to the WT mice, indicating a progressive increase in BACE1, as the AβPP mice aged (Table 2). BACE1 levels were lower in the 12- (−3.6-fold, $P < 0.005$) and 24-month-old (−1.4-fold) MCAT mice, relative to the WT mice. BACE1 levels were significantly lower in the 12- (−1.8-fold, $P < 0.05$) and 24-month-old (−1.9-fold, $P < 0.05$) MCAT/AβPP mice, relative to AβPP mice (Table 3).

APP levels were lower in the 12- and 24-month-old MCAT mice, relative to the WT mice. In contrast, APP levels were higher in the AβPP mice, relative to the WT mice in the same age groups. Further, the APP levels were lower in the 12- (−2.3-fold, $P < 0.05$) and 24-month-old (−1.5-fold) MCAT/AβPP mice, relative to the WT mice (Table 2) and were also significantly lower in the 12- (−2.3-fold, $P < 0.05$) and 24-month-old (−1.7-fold, $P < 0.05$) MCAT/AβPP mice, relative to the AβPP mice (Table 3).

As shown in Table 2, neprilysin mRNA levels were lower in the 6- (−1.2-fold), 12- (−1.4-fold, $P < 0.05$) and 24-month-old (−1.3-fold, $P < 0.05$) AβPP mice, relative to the WT mice. In contrast, the neprilysin levels were higher in the 6- (2.6-fold, $P < 0.05$), 12- (1.5-fold) and 24-month-old (1.3-fold) MCAT mice, relative to the WT mice. Neprilysin levels also were higher in the 6- (2.5-fold, $P < 0.05$), 12- (1.2-fold) and 24-month-old (1.5-fold, $P < 0.05$) MCAT/AβPP mice, relative to the WT mice. As shown in Table 3, neprilysin levels were significantly higher in the MCAT/AβPP mice, relative to the 6- (4.3-fold, $P < 0.05$), 12- (1.8-fold, $P < 0.05$) and 24-month-old (1.9-fold, $P < 0.05$) AβPP mice.

Table 3. mRNA fold changes of genes related to Aβ in 6-, 12- and 24-month-old MCAT/AβPP mice, relative to AβPP mice

Gene	mRNA fold change in 6-month-old MCAT/AβPP mice	mRNA fold change in 12-month-old MCAT/AβPP mice	mRNA fold change in 24-month-old MCAT/AβPP mice
Synaptophysin	5.3*	2.3*	4.3**
Catalase	5.4**	2.0*	2.1*
APP	−1.2	−2.3*	−1.7*
BACE1	−1.4	−1.8*	−1.9*
Neprilysin	4.3*	1.8*	1.9*
Insulin-degrading enzyme	1.7*	3.4**	1.9*
TTR	3.8**	2.2**	2.8**

*$P \leq 0.05$.
**$P \leq 0.005$.

Relative to neprilysin levels in the WT mice, the IDE levels in the MCAT and MCAT/AβPP mice were significantly higher, and relative to the WT mice, the IDE levels in the AβPP mice were significantly lower (Table 2). As shown in Table 3, IDE levels were higher in all three age groups in the MCAT/AβPP mice, relative to the AβPP mice.

TTR levels were significantly higher in all three age groups of the MCAT/AβPP mice, relative to the AβPP mice (Table 3). TTR levels were significantly higher in the 6- (2.6-fold, $P < 0.05$), 12- (2.1-fold, $P < 0.05$) and 24-month-old (1.9-fold, $P < 0.05$) MCAT/AβPP mice, relative to the WT mice (Table 2).

Catalase expression

To determine the expression and localization of catalase in the MCAT, MCAT/AβPP, AβPP and WT mice, we performed immunostaining analysis of catalase in the brain sections from 12- and 24-month-old mice from all four mouse groups. As shown in Supplementary Material, Figures S1 and S2, catalase-positive neurons were throughout the brain

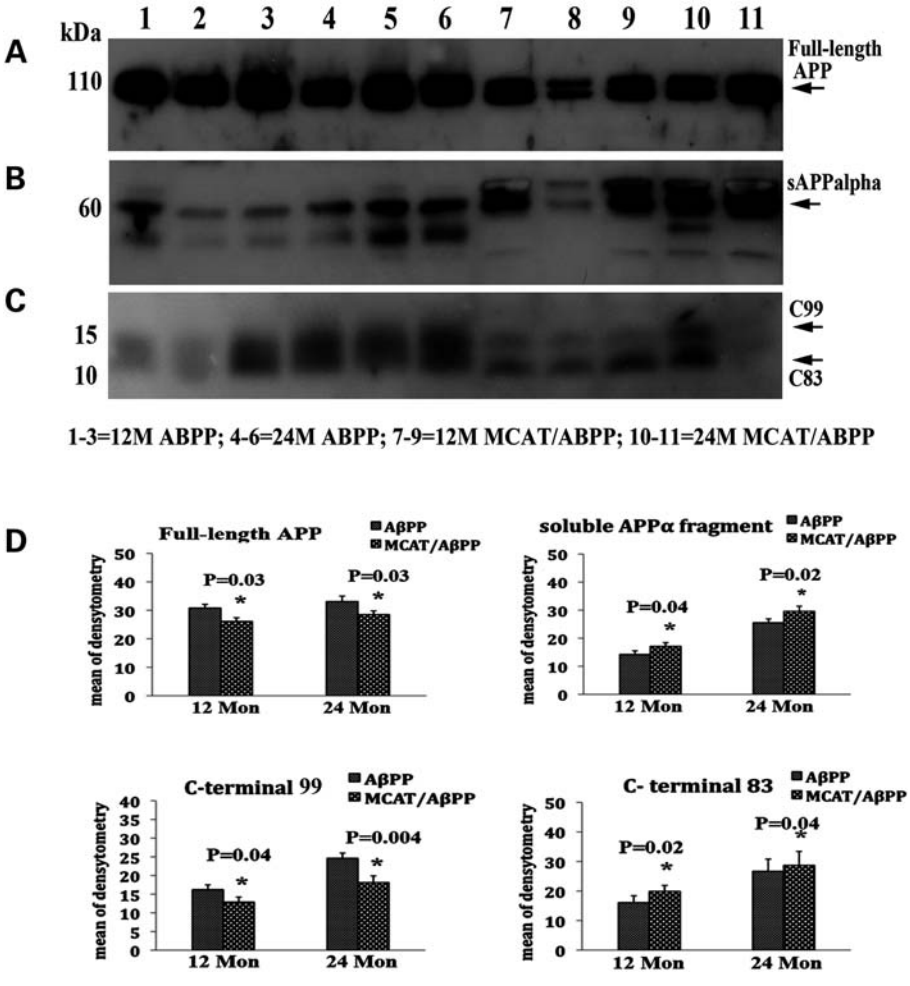

Figure 2. Western blot analysis of full-length AβPP, soluble APPα and C-terminal fragments CTF99 and CRTF83 in AβPP and MCAT/AβPP mice. (**A**) Immunoblotting analysis of full-length AβPP, (**B**) soluble APPα, (**C**) CTF99 and CTF83 and (**D**) densitometry quantification of proteins.

in all groups, indicating that catalase was widely expressed in the brain. However, our quantitative analysis revealed that the signal intensity of catalase immunoreaction was significantly higher in the 12- (Supplementary Material, Fig. S1, $P = 0.03$) and 24-month-old (Supplementary Material, Fig. S2, $P = 0.003$) MCAT mice, relative to the 12- and 24-month-old WT mice. A comparative analysis of the brain sections in AβPP and MCAT/AβPP mice in terms of catalase revealed significantly higher immunoreactive signal intensities in the 12- ($P = 0.03$) and 24-month-old ($P = 0.04$) MCAT/AβPP mice, relative to the AβPP mice. Further, catalase immunoreactivity was higher in the vicinity of Aβ deposits in the brain sections from the 24-month-old AβPP mice, indicating that catalase may decrease oxidative damage by scavenging free radicals in Aβ deposits.

MCAT reduces abnormal APP processing and elevates protective soluble APPα and CTF83 fragments

To determine the affects of MCAT in APP processing events, including the formation of soluble APPα, c-terminal fragments CTF99 and CTF83 and full-length APP, we performed immunoblotting analysis, using cortical lysates from 12- and 24-month-old AβPP and MCAT/AβPP mice. As shown in Figure 2A and D, we found significantly fewer full-length APP proteins in 12- ($P = 0.03$) and 24-month-old ($P = 0.03$) MCAT/AβPP mice, relative to the 12- and 24-month-old AβPP mice, indicating that MCAT interferes with age-dependent APP synthesis. However, we did not find a significant reduction in full-length APP in the 2-month-old MCAT/AβPP mice (data not shown).

We next quantified soluble APPα fragments in cortical lysates from 12- and 24-month-old AβPP and MCAT/AβPP mice. We found significantly more soluble APPα proteins in the 12- ($P = 0.04$) and 24-month-old ($P = 0.02$) MCAT/AβPP mice, relative to the 12- and 24-month-old AβPP mice (Fig. 2B and D), indirectly suggesting reduced BACE1 activity and/or increased α-secretase activity in the MCAT/AβPP mice.

As shown in Figure 2C and D, we found significantly fewer β-secretase-based c-terminal CTF99 fragments in the 12- ($P = 0.04$) and 24-month-old ($P = 0.004$) MCAT/AβPP mice, relative to the 12-month-old AβPP mice. As expected and in contrast, we found significantly higher α-secretase-based

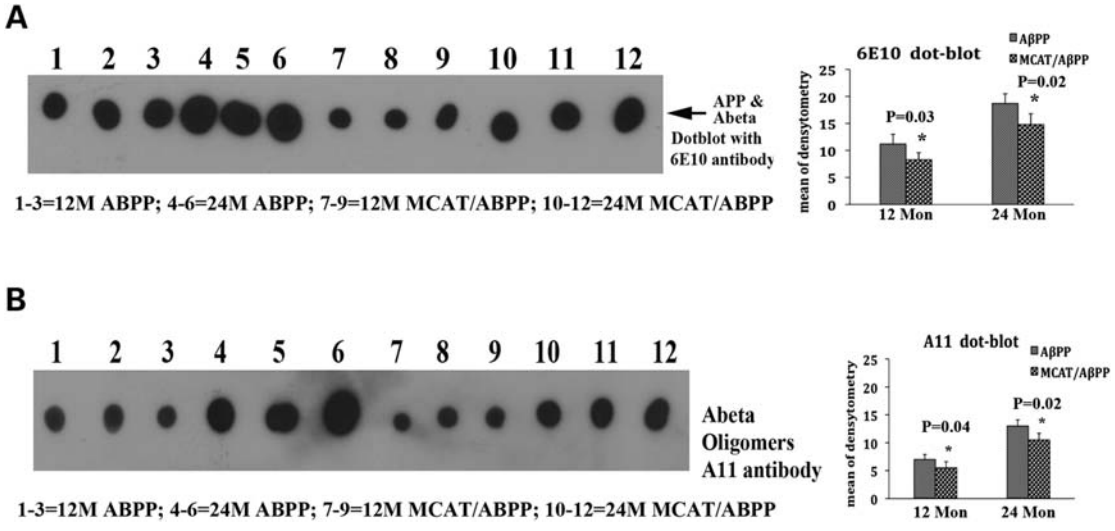

Figure 3. Dot blot analysis of AβPP and its derivatives and oligomeric Aβ in AβPP and MCAT/AβPP mice. (**A**) Dot blot analysis using the 6E10 Aβ antibody and (**B**) dot blot analysis using the oligomeric Aβ (A11) antibody. Significantly lower levels of AβPP and its derivatives and of oligomeric Aβ were found in the MCAT/AβPP mice relative to the AβPP mice.

c-terminal CTF83 fragments in the 12- ($P = 0.02$) and 24-month-old ($P = 0.04$) MCAT/AβPP mice, relative to the 12-month-old AβPP mice (Fig. 2C and D).

MCAT reduces APP derivatives and oligomeric Aβ

To determine whether MCAT reduces mutant APP derivatives and toxic oligomeric Aβ, we performed dot blot analyses, using cortical protein lysates from 12- and 24-month-old AβPP and MCAT/AβPP mice. As shown in Figure 3A, we found significantly fewer mutant APP derivatives that were immunoreactive to the 6E10 Aβ antibody in the 12- ($P = 0.03$) and 24-month-old ($P = 0.02$) MCAT/AβPP mice, relative to the AβPP mice. As shown in Figure 3B, we also found significantly less oligomeric Aβ in the 12- ($P = 0.04$) and 24-month-old ($P = 0.02$) MCAT/AβPP mice, relative to the AβPP mice.

Reduced Aβ levels in MCAT/AβPP mice

To determine whether MCAT alters Aβ levels in the brains of AβPP mice, we used sandwich enzyme linked immuno sorbant assay (ELISA) to analyze brain specimens from 6-, 12- and 24-month-old AβPP and MCAT/AβPP mice. As shown in Figure 4D, Aβ1-42 levels were significantly lower in the 12-month-old MCAT/AβPP mice (73.0 ± 4.9 pg Aβ42/mg protein), the 12-month-old AβPP mice (92.9 ± 7.5 pg Aβ42/mg protein; $P = 0.04$), the 24-month-old MCAT/AβPP mice (112.2 ± 8.1 pg Aβ42/mg protein) and the AβPP mice (139.4 ± 12.2 pg Aβ42/mg protein; $P = 0.04$), suggesting that MCAT is capable of decreasing Aβ42 levels during AD progression. Aβ40 was also lower in the 12- and 24-month-old MCAT/AβPP mice, relative to the AβPP mice (Fig. 4C). However, statistical significance was found only in results from the 24-month-old MCAT/AβPP (118.92 ± 7.3 pg Aβ42/mg protein) and the AβPP mice (149.0 ± 11.9 pg Aβ42/mg protein; $P < 0.05$). Further, an age-dependent increase in both Aβ40 (Fig. 4A) and Aβ42 (Fig. 4B) was found in the MCAT/AβPP and AβPP mice.

MCAT reduces Aβ plaques

To determine the effects of overexpressed MCAT on Aβ plaques in terms of their number and size, we used a 6E10 antibody that recognizes Aβ plaques derived from both Aβ40 and Aβ42. We determined the numbers and sizes of the Aβ plaques in the brain sections from the 12- and 24-month-old MCAT/AβPP mice and the age-matched AβPP mice. We found significantly fewer Aβ plaques in the 12- ($P < 0.005$; Fig. 5A) and 24-month-old ($P < 0.05$; Fig. 5B) MCAT/AβPP mice, relative to the AβPP mice. We also found significantly smaller Aβ plaques in the 12- ($P < 0.05$; Fig. 5A) and 24-month-old ($P < 0.05$; Fig. 5B) MCAT/AβPP mice, relative to the AβPP mice.

To determine whether MCAT is involved in reducing the longer or shorter form of Aβ, or both, we used Aβ40 and Aβ42 antibodies on the brain sections from MCAT/AβPP and AβPP mice. In sections immunostained with the antibody specific for Aβ42, significantly fewer Aβ plaques were found in the cortex and hippocampus brain sections, in the 24-month-old MCAT/AβPP mice ($P = 0.022$; Supplementary Material, Fig. S3), and the average size of the Aβ plaques was also significantly smaller in the 24-month-old MCAT/AβPP mice ($P = 0.041$), relative to the age-matched AβPP mice.

In sections immunostained with the Aβ40 antibody, Aβ plaques were significantly fewer in the brain sections from the 24-month-old MCAT/AβPP mice, relative to AβPP mice, but the Aβ plaques were not significantly smaller (Supplementary Material, Fig. S4).

MCAT reduces BACE1 enzymatic activity and protein levels

As shown in Figure 6A, the levels of BACE enzyme were significantly higher in 12- ($P = 0.03$) and 24-month-old

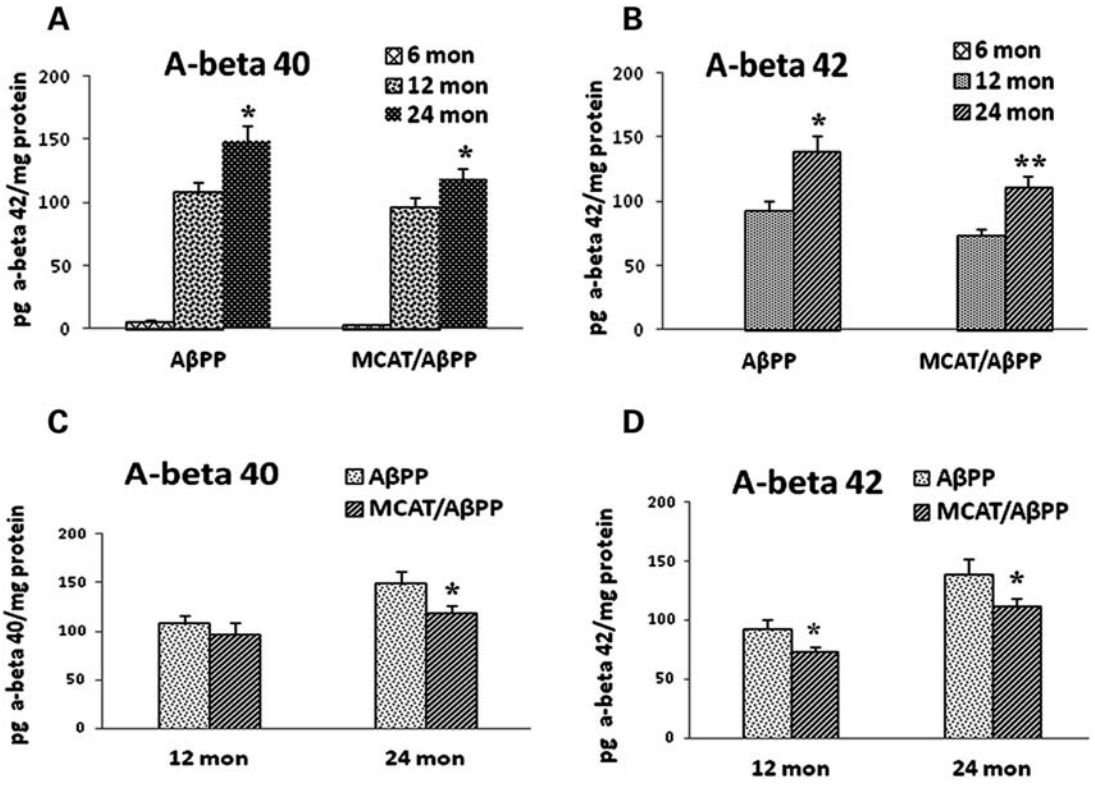

Figure 4. Aβ levels using sandwich enzyme linked immuno sorbant assay (ELISA) in brain sections from 6-, 12- and 24-month-old AβPP and MCAT/AβPP mice. Aβ40 and Aβ42 were quantified using sandwich ELISA and expressed as pg Aβ/mg protein. (**A**) Aβ40 levels in two transgenic lines at the three ages; (**B**) Aβ42 levels in two transgenic lines at the three ages; (**C**) Aβ40 levels in the MCAT/AβPP and AβPP mice and (**D**) Aβ42 levels in the MCAT/AβPP and AβPP mice.

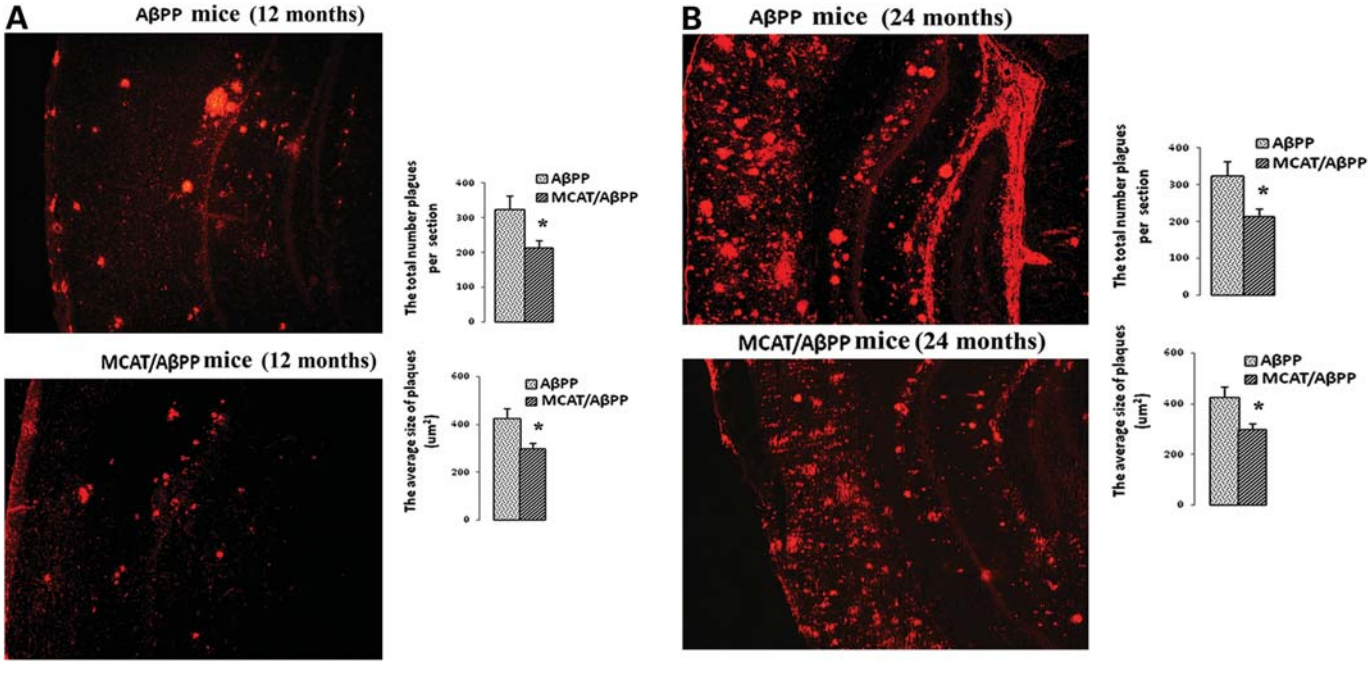

Figure 5. Aβ deposits in AβPP and MCAT/AβPP mice were assessed with the 6E10 monoclonal antibody. (**A**) Aβ deposits and quantification data in the 12-month-old AβPP and MCAT/AβPP mice. (**B**) Aβ deposits and quantification data in the 24-month-old AβPP and MCAT/AβPP mice. Images are with ×5 original magnification. The total number (upper) and size (bottom) of the Aβ plaques were significantly reduced in the 12- and 24-month-old MCAT/AβPP mice relative to the 12- and 24-month-old AβPP mice (*$P < 0.01$; four or five mice in each group).

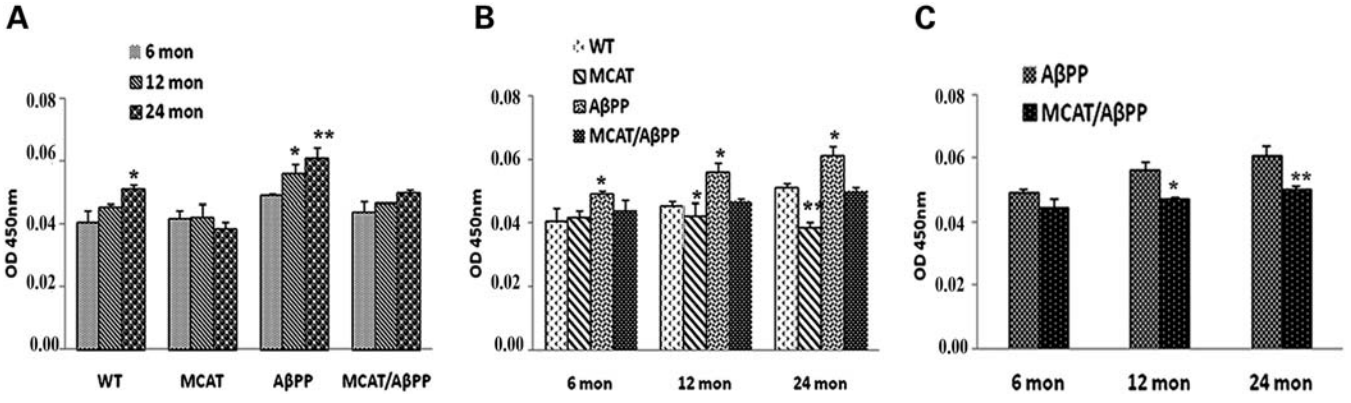

Figure 6. BACE1 enzymatic activity in the cortical and hippocampal tissues from the brains of transgenic and WT mice. (**A**) Changes in BACE1 activity of all four genotype groups ($^{*}P < 0.05$; $^{**}P < 0.005$). (**B**) Differences across the ages ($^{**}P < 0.005$). (**C**) Difference in BACE1 activity in the AβPP and MCAT/AβPP mice at the three ages ($^{**}P < 0.005$).

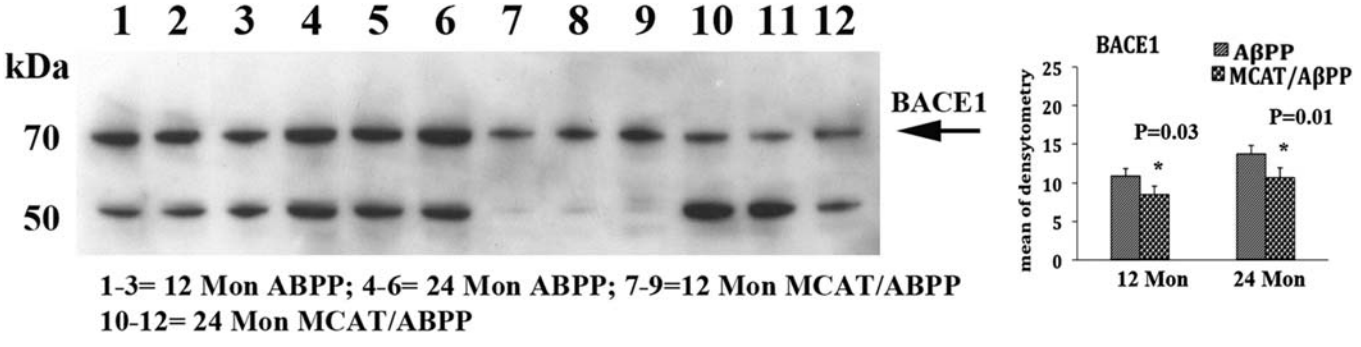

Figure 7. Western blot analysis of BACE1 in the 12- and 24-month-old AβPP and MCAT/AβPP mice. Significantly lower level of BACE1 protein was found in the MCAT/AβPP mice, relative to the AβPP mice.

($P = 0.001$) AβPP mice, relative to the 6-month-old AβPP mice. In the WT mice also, BACE activity increased with age, but it significantly increased in the 24-month-old ($P = 0.03$) WT mice, relative to 6-month-old mice. The levels of the BACE1 enzyme were also significantly higher in the brain sections from the AβPP mice than the WT mice (Fig. 6B) for the 6- ($P = 0.03$), 12- ($P = 0.01$) and 24-month-old ($P = 0.02$) mice. The BACE1 enzyme was significantly higher in the brains of the 12- ($P = 0.04$) and 24-month-old ($P = 0.001$) MCAT mice, compared with the age-matched WT mice (Fig. 6B). Perhaps more importantly, BACE levels in the MCAT/AβPP mice were significantly lower, relative to the levels in the AβPP mice (Fig. 6C, $P = 0.04$) and the MCAT/AβPP mice at 12 months ($P = 0.001$), relative to the MCAT/AβPP mice at 24 months. As shown in Figure 6A, the levels of BACE1 were higher in an age-dependent manner in the AβPP and WT mice, indicating that age may play a large role in enhancing BACE1 levels and producing higher Aβ levels.

To determine whether MCAT reduces BACE1 proteins in the MCAT/AβPP mice, we performed immunoblotting analyses and quantified BACE1 proteins in 12- and 24-month-old AβPP and MCAT/AβPP mice. As shown in Figure 7, we found significantly lower quantities of the BACE1 protein in the 12- ($P = 0.03$) and 24-month-old ($P = 0.01$) MCAT/AβPP mice, relative to the 12- and 24-month-old AβPP mice, indicating that MCAT may interfere with BACE1 activity and protein levels in the MCAT/AβPP mice.

We also conducted quantitative immunohistochemistry analyses of BACE1 in the brain sections from the 12- and 24-month-old MCAT, AβPP, MCAT/AβPP and WT mice. We found that the immunoreactive signal intensity of BACE1 was higher in the 12- ($P = 0.01$, Supplementary Material, Fig. S5) and 24-month-old ($P = 0.001$, Supplementary Material, Fig. S6) AβPP mice, relative to the 12- and 24-month-old WT mice. Our comparative analysis of BACE1 immunoreactivity in the AβPP and MCAT/AβPP mice revealed that its immunoreactive signal intensity was significantly less in the 12- (Supplementary Material, Fig. S5D and H) and 24-month-old (Supplementary Material, Fig. S6D and H) MCAT/AβPP mice, relative to the 12- (Supplementary Material, Fig. S5C and G) and 24-month-old (Supplementary Material, Fig. S6C and G) AβPP mice, suggesting that MCAT appears to play a large role in decreasing BACE levels in mice expressing Aβ.

MCAT reduces oxidative DNA damage in the mouse brain

Using 8-hydroxy-2-deoxyguanosine (8-OHdG), a marker for oxidative DNA damage, we analyzed oxidative DNA damage in genomic DNA prepared from cerebral cortices of the AβPP, MCAT, MCAT/AβPP and WT mice, at three ages 6,

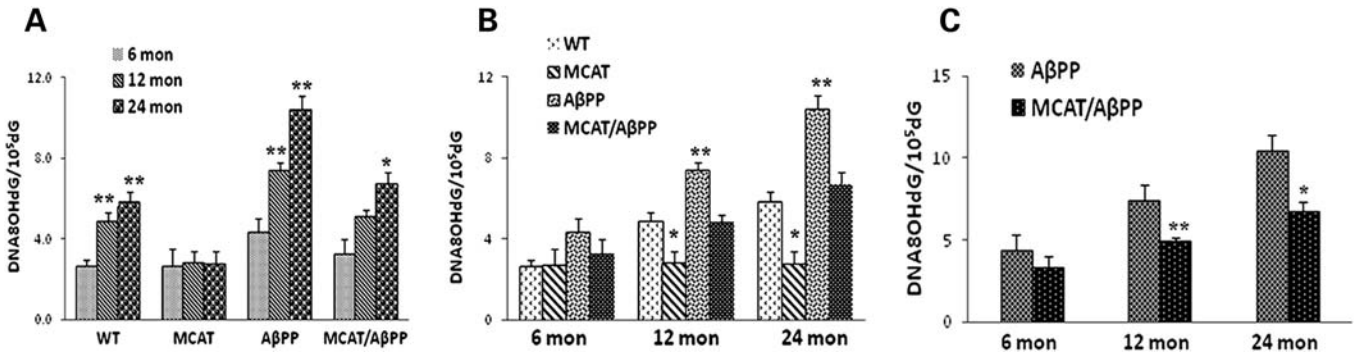

Figure 8. 8-OHdG quantification, using high pressure liquid chromatography (HPLC) analysis of the cortical and hippocampal tissues from the brains of transgenic and WT mice. (**A**) Changes in the levels of 8-OHdG in all four genotype groups ($^{*}P < 0.05$; $^{**}P < 0.005$). (**B**) Differences across the ages ($^{*}P < 0.05$). (**C**) Levels of 8-OHdG in the AβPP and MCAT/AβPP mice at the three ages ($^{*}P < 0.05$; $^{**}P < 0.01$).

12 and 24 months. Figure 8 gives data on 8-OHdG levels, represented as OHdG/10^5dG. The levels of 8-OHdG were significantly higher in the 12- (4.9 ± 0.41; $P = 0.002$) and 24-month-old (2.7 ± 0.26; $P = 0.001$) WT mice, relative to the 6-month-old WT mice, indicating the presence of age-dependent oxidative DNA damage (Fig. 8A). However, in the MCAT mice, 8-OHdG levels were unchanged in the 12- and 24-month-old mice, relative to the 6-month-old mice (Fig. 8A), indicating that MCAT may prevent age-related oxidative DNA damage. Similar to the WT mice, 8-OHdG levels in the 12- (6-month AβPP mice 4.3 ± 0.66 and 12-month AβPP mice 7.4 ± 0.38, $P = 0.003$) and 24-month-old AβPP mice (6-month AβPP mice 4.3 ± 0.66 OHdG/10^5dG and 24-month AβPP mice 10.6 ± 0.67, $P = 0.001$) significantly increased, relative to the 6-month-old AβPP mice (Fig. 8A). The 8-OHdG levels were significantly lower in the 12- (2.8 ± 0.55, $P = 0.02$) and 24-month-old (2.8 ± 0.58, $P = 0.01$) MCAT mice than in the 12- (4.9 ± 0.41) and 24-month-old (5.8 ± 0.52) WT mice (Fig. 8B). As shown in Figure 8C, the 8-OHdG levels were significantly lower in the MCAT/AβPP mice at 12 (12-month AβPP mice, 7.4 ± 0.38; 12-month MCAT/AβPP mice, 5.1 ± 0.33; $P = 0.01$) and 24 months of age (24-month AβPP mice, 10.4 ± 0.67; 24-month MCAT/AβPP mice, 6.7 ± 0.61; $P = 0.002$), relative to the age-matched AβPP mice, indicating that MCAT may significantly reduce oxidative damage to the DNA in brain neurons.

To better understand the role of MCAT in oxidative DNA damage, we used the 8-OHdG antibody and immunohistochemistry to characterize the immunoreactivity of 8-OHdG in 12- and 24-month-old MCAT, AβPP, MCAT/AβPP and WT mice. 8-OHdG immunoreactivity was significantly higher in the 12- (Supplementary Material, Fig. S7C and G; $P = 0.02$) and 24-month-old (Supplementary Material, Fig. S8C and G; $P = 0.01$) AβPP mice, relative to the 12- (Supplementary Material, Fig. S7A and E) and 24-month-old WT mice (Supplementary Material, Fig. S8A and E). Our comparative analysis of 8-OHdG immunoreactivity in the brain sections from the AβPP and MCAT/AβPP mice revealed that the immunoreactive signal intensity of 8-OHdG was significantly less in the 12- (Supplementary Material, Fig. S7, $P = 0.04$) and 24-month-old (Supplementary Material, Fig. S8, $P = 0.03$) MCAT/AβPP mice, relative to the AβPP mice, suggesting that MCAT appears to play a role in decreasing oxidative DNA damage in neurons affected by AD in mice.

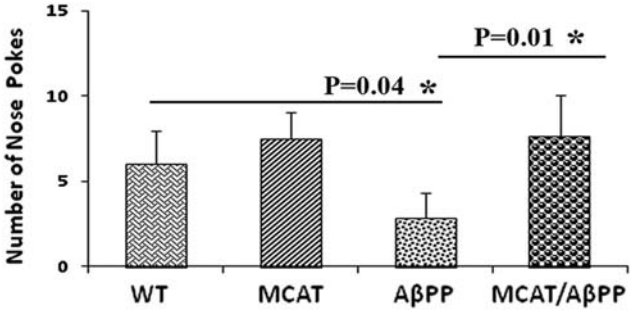

Figure 9. Assessment of cognitive behavior in transgenic and WT mice. Data were expressed as the mean ± SD ($^{*}P < 0.05$).

MCAT improves cognitive behavior

To understand the effects of MCAT on the hippocampus-related working memory of AβPP mice, we used the nose poke test (32–36) in the 12-month-old MCAT, AβPP, MCAT/AβPP and WT mice. Not surprisingly, after all four groups of mice received training followed by three trials of nose pokes, the MCAT/AβPP mice exhibited significantly increased counts of food nose poking relative to the AβPP mice ($P = 0.01$; Fig. 9), indicating that MCAT enhanced the working memory in the MCAT/AβPP mice. Further, the AβPP mice also showed significantly decreased nose poking relative to the WT mice ($P = 0.04$), suggesting that the nose-poke test is a reliable test for determining memory and cognitive functions in mice, since the AβPP mice have been reported to have memory and cognitive deficits (31).

DISCUSSION

The objective of our study was to investigate the protective effects of MCAT from birth to death, in mice that express Aβ. Using immunoblotting and immunostaining analyses, we studied the production of full-length APP; soluble APPα; C-terminal fragments CTF99 and CTF83; oligomeric Aβ; Aβ40, Aβ42 and Aβ deposits and BACE1 in different

stages of disease progression in MCAT/AβPP and AβPP mice. Using quantitative RT–PCR and immunostaining analyses, we also studied the expression of catalase, AD markers, synaptophysin, APP, the Aβ-degrading enzyme neprilysin, the insulin-degrading enzyme and Aβ-sequester TTR in MCAT, AβPP, MCAT/AβPP and WT mice. To determine the effect of MCAT on oxidative DNA damage, we measured the levels of 8-OHdG in the cerebral cortex of MCAT, AβPP, MCAT/AβPP and WT mice. We found that MCAT reduced the levels of full-length APP, Aβ (monomers and oligomers) and Aβ plaques and increased the levels of soluble APPα and α-secretase-based CTF83 in the MCAT/AβPP mice. Interestingly, the Aβ-degrading enzyme neprilysin and the insulin-degrading enzyme were elevated in the MCAT/AβPP mice. Finally, MCAT extended the lifespan of MCAT/AβPP mice (Fig. 1).

MCAT and lifespan extension

To determine whether the expression of MCAT modulates the healthy lifespan of AβPP transgenic and WT mice, we analyzed mortality data of these mouse lines from birth to death. The MCAT transgenic mice had an extended median lifespan of 4 months compared with the WT mice. Interestingly, the median lifespan of mice with the AβPP mutation was 5 months shorter than that of non-transgenic WT mice, and the maximum lifespan of mice with the AβPP mutation was reduced by 3.5 months, indicating that the AβPP mutation may responsible for the premature death of the AβPP mice that we found (Fig. 1). Further, the MCAT/AβPP mice had a median lifespan that was 4 months longer than that of the AβPP mice, indicating that MCAT decreased Aβ-related toxicities and complications and extended the lifespan of mice carrying the AβPP mutation. Further, greater percent of MCAT female mice lived longer than MCAT male mice, suggesting that MCAT scavenges free radicals and reduces age-related oxidative insults, protects and extends lifespan of female mice better than male mice. It would be interesting to see, if MCAT extends the lifespan of female MCAT/AβPP mice better than male MCAT/AβPP mice. However, the definite conclusion could not be drawn in the current study because numbers of female and male MCAT/AβPP mice studied for lifespan were small, and this issue may be addressed in the future study with a large number of female and male MCAT/AβPP mice relative to a large number of female and male AβPP mice. Addressing this issue is critical and important to develop mitochondria-targeted therapeutic strategies for male and female AD patients.

In the mortality data of the MCAT, AβPP, MCAT/AβPP and WT mice, multiple factors were found to be responsible for their death. However, the vast majority of mice in all four mouse lines died of tumors. Interestingly, some AβPP animals died prematurely, before 4 months of age. This premature death was not observed in the MCAT/AβPP mice, indicating that MCAT protects against Aβ and age-related toxicity.

To determine whether MCAT ameliorates cognitive deficits, particularly olfactory-related memory in AD, we studied the cognitive behavior of the MCAT/AβPP and AβPP mice with the nose-poke test. Findings from previous lesion studies indicated that the integrity of the hippocampal formation is essential for normal working memory (37). AD patients, as well as AD-like mice, clearly show memory deficits and olfactory-related memory disorders due to damage in the hippocampus and cortex (36,38,39). The increased targeted nose pokes that were observed in the MCAT/AβPP mice, relative to the AβPP mice, suggest that MCAT significantly increased working memory in AβPP mice.

Aβ-related gene expressions and MCAT

To determine the effect of MCAT on aging and Aβ, we performed a time-course, gene-expression analysis of several AD-related genes, using RNA from the cerebral cortex of MCAT, AβPP, MCAT/AβPP and WT mice at 6, 12 and 24 months of age. As expected, we saw reduced mRNA levels of Aβ-degrading enzymes, neprilysin, insulin-degrading enzyme and synaptophysin and catalase in the AβPP mice, relative to the WT mice, at each of the three ages. However, these genes were progressively up-regulated in the MCAT and MCAT/AβPP mice, indicating that MCAT enhances neprilysin, insulin-degrading enzyme and synaptophysin and protects neurons from toxic insults of aging and Aβ, since MCAT is known to scavenge free radicals (30) and to clear toxic metabolites produced by free radicals.

Interestingly, mRNA expressions of the AD-induced genes APP and BACE1 progressively increased in the AβPP mice as they aged, relative to the WT mice, and APP and BACE1 were down-regulated in the MCAT and MCAT/AβPP mice. These results suggest that MCAT plays a critical role in lowering APP and BACE1 expressions as the AβPP mice age and, by extension, as AD progresses and that age- and Aβ-dependent free radicals may be critical for the elevated levels of APP and BCAE1 found in the AβPP mice as AD progresses. Our results also support mitochondria-targeted molecules protecting neurons from age- and Aβ-induced toxic insults.

Abnormal APP processing and MCAT

One purpose of our study was to better understand the role of MCAT in APP processing during disease progression in AβPP mice. To this end, we measured full-length APP, soluble APPα and c-terminal fragments resulting from the cleavage of APP molecules (β-, α- and γ-secretases). We found significantly decreased levels of full-length APP and β-secretase-based CTF99 and increased levels of soluble APPα and α-secretase-based CTF83 in 12- and 24-month-old MCAT/AβPP mice relative to AβPP mice. These results indicated that MCAT interferes with APP processing and reduces Aβ production.

To determine mechanisms underlying the beneficial effects of MCAT overexpression, we examined whether MCAT affected the production and accumulation of Aβ in the brains of the MCAT/AβPP mice. We stained sections from the mouse brains of the MCAT/AβPP and AβPP mouse lines, using the 6E10 Aβ antibody, which recognizes both full-length APP and its derivatives. MCAT reduced the 6E10-stained Aβ plaque burden in the 12- and 24-month-old MCAT/AβPP mice. Since Aβ42 is more toxic than the other forms of Aβ, we further examined the levels of Aβ40 and Aβ42 in brain slices from the MCAT/AβPP and AβPP

mice, using end-specific monoclonal antibodies against Aβ40 and Aβ42. MCAT dramatically reduced both Aβ40- and Aβ42-derived plaques, especially the Aβ42-derived plaques in terms of their quantity and average size.

Our quantitative dot blot analyses of Aβ oligomers (using the A11 antibody), APP and APP derivatives (using 6E10 antibody) revealed significantly reduced APP, APP derivatives and Aβ oligomers in the MCAT/AβPP mice, confirming that MCAT reduces full-length APP and toxic derivatives of APP during disease progression.

These findings clearly support the protective role of MCAT and its likely involvement in reducing Aβ plaques in the MCAT/AβPP mice.

BACE1 and MCAT

Aβ is produced by the cleavage of AβPP via BACE1 and γ-secretase, and BACE1 is the enzyme that initiates a proteolytic reaction and produces Aβ. Notably, BACE1$^{-/-}$ mice are the devoid of Aβ, demonstrating that BACE1 is the major, if not the only, β-secretase producing enzyme in the brain (40). BACE1 is highly expressed in the AD brain and AD transgenic mouse models, suggesting that an increase in BACE1 might accelerate AD pathogenesis (41). Genetic deletion of BACE1 reduces soluble Aβ oligomers and rescues both temporal and spatial memory deficits in APP transgenic mice (42). Our data also showed that BACE1 expression is higher in the AβPP transgenic mice, relative to the age-matched WT mice. Interestingly, we found that MCAT significantly inhibits BACE1 expression in WT and AβPP mice, as determined by quantitative immunoblotting and immunohistochemistry. Even though the detailed mechanisms of reduced BACE1 expression in MCAT/AβPP mice are unknown, previously it was shown that oxidative stress, ischemia, hypoxia and ischemia increase BACE1 expression levels (43–46), ROS and the oxidative stress was less in MCAT transgenic mice. Reduced BACE1 expression and activity in MCAT mouse brain, and then as a consequence result, a reduced Aβ production occurred in MCAT/AβPP mice.

Oxidative stress, Aβ, AD and MCAT

Amyloid β accumulation has been reported in both early onset familial AD and late-onset sporadic AD. In early onset familial AD, genetic mutations in APP, PS1 and PS2 genes activate both β- and γ-secretases and produce Aβ. In contrast, in late-onset sporadic AD, age-related oxidative stress in the brain activates β- and γ-secretases and produces Aβ. This age-related brain oxidative stress causes disease progression later in life (3,6,12). Irrespective of whether Aβ is produced by genetic mutation (in familial AD) or oxidative stress and other factors (in sporadic AD), as we found in the present study, mitochondria-targeted catalase scavenges free radicals that are generated within the mitochondria and may lower BACE1 and γ-secretase, may reduce Aβ and its associated toxic insults, may protect neurons and may extend lifespan. Therefore, MCAT likely protects against age-related oxidative stress and Aβ-induced toxicities in AD progression.

Free radicals and MCAT

As discussed above, in familial AD, Aβ toxicity is mediated, at least in part, by oxidative stress. Aβ directly generates ROS in the presence of iron or copper ions (47). Further, H_2O_2 is generated during the very early stages of amyloid peptide aggregation (48). Aβ oligomers also induce neuronal oxidative stress through *N*-methyl-D-aspartate receptors and calcium influx (49). Interestingly, it has been shown that the administration of exogenous catalase prevented Aβ- and H_2O_2-mediated neuron death in rat cortical neuron cultures (50,51). Thus, catalase increases the resistance of cultured neurons to Aβ-induced toxicity by decreasing oxidative stress. Overall, mitochondria-targeted antioxidants protect neurons against Aβ-induced oxidative insults.

The overexpression of MCAT in mice markedly reduces ROS and lipid peroxidation, attenuates murine cardiac aging (30,52,53) and prevents age-dependent reductions in mitochondrial function and insulin resistance (54,55). Our results indicate that MCAT overexpression reduces age- and Aβ-induced Aβ production, abnormal APP processing events in the MCAT/AβPP mouse brain. Therefore, MCAT overexpression also increases resistance to Aβ-induced toxicity *in vivo*. Transgenic mice overexpressing MCAT showed increased catalase, which converted H_2O_2 to water and oxygen, thereby reducing oxidative stress. In fact, we observed decreased brain DNA oxidation in MCAT mice, compared with age-matched WT mice, and MCAT/AβPP mice, compared with age-matched AβPP mice. The increase in lifespan, in both MCAT and MCAT/AβPP mice may be directly attributable to the protective role of MCAT. However, the extended, healthy lifespan of the MCAT/AβPP mice was similar to that of the WT mice, suggesting that MCAT significantly reduced Aβ production and plaques, which, in turn, increased the lifespan of the AβPP mice.

Oxidative DNA damage and MCAT

Oxidative DNA damage has been extensively investigated in affected brain tissues from AD patients (56–60). Increased free radical production, produced from either mitochondria or an inflammation process (macrophage or microglia in the brain), can cause oxidation of nucleic acids, especially DNA. The resulting DNA damage is present in AD and in aging (5). Further, the Aβ42 peptide showed more DNA nicking and causing direct oxidative DNA damage in AD-affected neurons. The levels of multiple, oxidized bases in AD patients were significantly higher in the frontal, parietal and temporal lobes compared with levels in the control subjects. In contrast, the cerebellum was only slightly affected in the AD brains. mtDNA had levels of oxidized bases that were ∼10-fold higher than those of nDNA in the AD brains (60).

In the present study, we found significantly higher levels of 8-OHdG in the 12- and 24-month-old WT mice, relative to the 6-month-old WT mice, indicating that aging may be involved in enhancing oxidative DNA damage. In contrast, in the MCAT mice, 8-OHdG levels were unchanged in the 12- and 24-month-old mice, relative to the 6-month-old mice, suggesting that MCAT prevents oxidative DNA damage. More importantly, we found significantly higher 8-OHdG levels at all

three time-points of investigation, in AβPP mice that we studied, indicating that Aβ overexpression may elevate DNA damage. However, 8-OHdG levels were markedly lower at all time-points in the MCAT/AβPP mice, relative to the AβPP mice, directly indicating that MCAT may protect against Aβ and age-related brain oxidative damage.

In summary, our results suggest that oxidative stress is involved in aging and in the progression and pathogenesis of AD, that MCAT suppresses brain oxidative damage and toxic Aβ production and accumulation and that MCAT enhances α-secretase-based soluble APPα and CTF83 fragments. Thus, MCAT may be a potential therapeutic agent to prevent or to treat AD in elderly individuals.

MATERIALS AND METHODS

Mice and tissue preparation

To study the protective effects of MCAT, we used AβPP transgenic mice (Tg2576 mouse line; gifted by Karen Ashe, PhD, University of Minnesota) (31) and MCAT mice (30).

The AβPP mice

The AβPP mice were generated with the mutant human APP gene 695-amino-acid isoform and a double mutation ($Lys^{670}Asn$ and $Met^{671}Leu$) (31). The AβPP mice and their non-transgenic WT littermates were maintained on a C57BL6/SJL background. The AβPP mouse model exhibits age-dependent Aβ plaques as well as a distribution of Aβ plaques in the cerebral cortex and the hippocampus, but not in the striatum, the deep gray nuclei and the brain stem. Disease in this mouse model parallels AD in that elevated amounts of soluble Aβ correlate with increased free-radical production, and the Aβ plaques evoke a microglial reaction in their immediate vicinity (19,61).

The MCAT mice

MCAT mice were generated by conventional microinjection techniques into BL6 embryos. The founder lines were back-crossed onto the BL6 background and maintained as described previously (30).

Generation of double transgenic mice

We generated the double transgenic mice by crossing AβPP mice with MCAT mice. Genotyping was performed by PCR on genomic DNA, using specific transgenic primers (APP forward: 5′-CTGACCACTCGACCAGGTTCTGGG, reverse: 5′-GTCGATAACCCCTCCCCCAGCCTAGACCA; MCAT forward: 5′-CTGAGGATCCTGTTAAACAATGC, reverse: 5′-GAAGTCCCAGACCATGTCCGGAT or 5′-GGGAAAGT CTCGCCGCATCTTC). Another three lines of genotype (MCAT, AβPP and WT) were also obtained from the crossing and routine PCR. All experimental mice were single-caged in a humidity- and temperature-controlled room, with 12-h light/dark cycles. All procedures were performed during the light cycle and were approved by the Institutional Animal Care and Use Committee (IACUC) at Oregon Health and Science University.

About 150 transgenic and WT littermates from 3 to 37 months were randomly distributed among four different groups. At the end of the experiments, the mice were euthanized and the brains excised for DNA isolation and for histological, biochemical and quantitative analyses. For lifespan analysis, we maintained the transgenic and WT mice until death or a request for euthanization was made by an animal caretaker or veterinarian. This approach ensured that the lifespan data reflected the animal's lifespan in our experiments.

Real-time RT–PCR quantification of mRNA expression of synaptophysin, catalase, BACE1, APP, Aβ-degrading enzymes and TTR

To determine whether MCAT and aging alter mRNA levels of catalase, synaptophysin, APP, BACE1 and Aβ-degrading enzymes, we performed real-time RT–PCR analysis using total RNA from 6-, 12- and 24-month-old MCAT, AβPP, MCAT/AβPP and WT mice. We prepared total RNA using the reagent TRIzol (Invitrogen, Temecula, CA, USA). We used Primer Express Software (Applied Biosystems, Foster City, CA, USA) to design the oligonucleotide primers for the housekeeping genes β-actin and glyceraldehyde-3-phosphate dehydrogenase, catalase, synaptophysin, APP, BACE1, neprilysin, insulin-degrading enzyme and TTR. The primer sequences and amplicon sizes are given in Table 4. Using SYBR-Green, chemistry-based quantitative real-time RT–PCR, we measured mRNA expression in our study genes, following Manczak *et al*. (61) and Shirendeb *et al*. (62).

Western blot analysis

To determine whether MCAT affects APP processing and alters full-length APP, APP derivatives and BACE1, using the standard western blotting analysis described in Manczak *et al*. (26), we performed immunoblotting analysis with proteins prepared from cortical tissues from the AβPP and MCAT/AβPP mice. Briefly, 50 μg of protein lysates was resolved on 10–20% Tricine PAGE gel (Invitrogen). The resolved proteins were transferred to polyvinylidene fluoride membranes (Millipore, San Diego, CA, USA) and then were incubated for 1 h at room temperature with a blocking buffer [5% dry milk dissolved in the tris buffered saline with tween-20 (TBST) buffer]. The membranes were incubated overnight with the primary antibodies to detect full-length APP (APP rabbit polyclonal antibody, 1:500; Abcam, Cambridge, MA, USA), soluble APPα, CTF99 and CTF83 fragments (C-terminal APP rabbit polyclonal antibody, 1:400; Millipore) and BACE1 (dilution, 1:400, rabbit polyclonal; Calbiochem, San Diego, CA, USA). Details of antibody dilutions are given in Table 5. Proteins were detected with chemiluminescent reagents (Pierce Biotechnology, Rockford, IL, USA), and the bands from immunoblots were quantified on a Kodak scanner (ID Image Analysis Software, Kodak Digital Science, Kennesaw, GA, USA). Briefly, image analysis was used to analyze gel images captured with a Kodak Digital Science CD camera. The lanes were marked to define positions and specific regions on the bands. An ID fine-band command was used to locate and to scan the bands in each lane and to record the readings. Using ImageJ analysis, we analyzed the intensity of the bands and assessed statistical significance using the Student's *t*-test with a significance level

Table 4. Summary of real-time RT–PCR mouse primers used in measuring mRNA expression of Aβ-related genes

Markers	DNA sequence (5′–3′)	PCR product size (bp)
Catalase	Forward primer: CCCTCGGACTTTGGCAAA Reverse primer: CCAGACTCGAGTATCGCTGACA	55
Synaptophysin	Forward primer: CATTCAGGCTGCACCAAGTG Reverse primer: TGGTAGTGCCCCCTTTAACG	59
BACE1	Forward primer: TCCGGCTCAGAACTACAGTGTAAT Reverse primer: TGCGGCGTTTTCATGGT	58
Aβ	Forward primer: GTGGATAACCCCTCCCCCAGCCTAACCA Reverse primer: CTGACCACTCGACCAGGTTCTGGGT	60
Neprilysin	Forward primer: GAGCCCCTTACTAGGCCTGTGT Reverse primer: CTCGATTCAGACATAGGCTTTCTAAA	66
Insulin-degrading enzyme	Forward primer: CCGGCCATCCAGAGAATAGAA Reverse primer: ACGGTATTCCCGTTTGTCTTCA	69
TTR	Forward primer: TGGACACCAAATCGTACTGGAA Reverse primer: CATCCGCGAATTCATGGAA	59
β-Actin	Forward primer: ACGGCCAGGTCATCACTATTC Reverse primer: AGGAAGGCTGGAAAAGAGCC	65

of $P < 0.05$. Western blot band intensities were expressed as the mean ± SD.

Dot blot analysis of Aβ and Aβ oligomers

To determine whether MCAT alters APP and its derivatives, including Aβ and Aβ oligomers, in MCAT/AβPP mice, we performed dot blot analysis using 6E10 and A11 antibodies and cortical lysates from AβPP and MCAT/AβPP mice as described in Shirendeb *et al*. (62). Briefly, 10 μg of protein from cortical tissues from AβPP and MCAT/AβPP mice was spotted onto a nitrocellulose membrane that was then air-dried for 1 h. The membranes were soaked in 5% milk in TBST for 1 h to block non-specific sites and were then incubated with the Aβ antibodies, 6E10 (dilution 1:300, mouse monoclonal; Covance, San Diego, CA, USA), and an oligomeric-specific antibody (A11, anti-rabbit polyclonal, 1:200; Invitrogen) in the blocking solution for 1 h at room temperature. Details of antibodies are given in Table 5. The membranes were washed three times with TBST and then incubated with an appropriate secondary antibody that was conjugated with HRP (horseradish peroxidase; 1:10 000 dilution) for 30 min at room temperature. The membrane was again washed three times with TBST and incubated with the enhanced chemiluminescence reagent for 1 min before it was exposed to the X-ray film. Using ImageJ analysis, we quantified Aβ- and oligomer-specific dots from dot blots and assessed statistical significance with the student's *t*-test.

DNA isolation and HPLC analysis of DNA damage

To determine the effects of MCAT on oxidative DNA damage, we measured hydroxy-2′-deoxyguanosine (oxidized DNA) in slices from the cerebral cortex and hippocampal regions of the 6-, 12- and 24-month-old MCAT, AβPP, MCAT/AβPP and WT mice. We isolated total genomic DNA from frozen samples of the cerebral cortex and hippocampal regions of the 6-, 12- and 24-month-old MCAT, AβPP, MCAT/AβPP and WT mice, using phenol extraction and ethanol precipitation procedures described in Laws and Adams (63) and Lau *et al*. (64). Briefly, 50 mg of frozen tissue was homogenized in 500 μl of cold 10 mM ethylenediaminetetraacetic acid (EDTA) (pH 8.0) through a glass homogenizer. The homogenate was incubated with 5 μl of RNase A (Ambion Inc.) and 5 μl of RNase T1 (Ambion Inc.) in an Eppendorf tube for 1 h at 37°C. Subsequently, proteins were digested by adding 34 μl of 20% SDS, 35 μl of 1 M Tris (pH 7.5) and 12 μl of proteinase K (Ambion Inc.) and then incubated for 1 h at 37°C. The incubation mixture was transferred to an Eppendorf tube. Tris–HCl saturated phenol (750 μl) was added and mixed by vortexing and was then centrifuged. The aqueous phase was transferred to an Eppendorf tube, and DNA was extracted with 300 μl of phenol/chloroform/isoamyl alcohol (25:24:1, v/v) and washed with 300 μl of chloroform/isoamyl alcohol (24:1, v/v). DNA was precipitated with 0.14 M sodium acetate and 50% (v/v) isopropanol, washed once with 100 μl of 70% ethanol and redissolved in 250 μl of 1.0 mM EDTA. The RNase, proteinase K and extraction steps were repeated once for greater purity. The DNA was collected by centrifugation, washed twice with 70% ethanol and resuspended in 150 μl of 1.0 mM EDTA, pH 8.0. The purity and concentration of DNA were determined spectrophotometrically.

The total DNA was digested and dephosphorylated by nuclease P1, followed by alkaline phosphatase. Digested DNA was analyzed by high pressure liquid chromatography (HPLC) equipped with a reverse-phase analytical column. DNA was then coupled with a photodiode array detector (SPD-M10A, Shimadzu, Columbia, MD, USA), followed by an electrochemical detector (CoulArray, ESA, Chelmsford, MA, USA). Quantification of nucleosides was by EC at 254 nm while the electrochemical detector (at 290 mV) measured 8-oxo-dG.

Measurement of soluble Aβ levels in AβPP and MCAT/AβPP mice

The cerebral cortex of each mouse brain was snap-frozen on dry ice at the time of sacrifice and stored at −70°C until a homogenate was prepared according to Manczak *et al*. (19).

Table 5. Summary of antibody dilutions and conditions used in immunoblotting analysis of proteins in transgenic mice and WT mice

Marker	Primary antibody Species and dilution	Purchased from	Secondary antibody Dilution	Purchased from
BACE1	Rabbit polyclonal 1:400	Calbiochem, San Diego, CA, USA	Donkey anti-rabbit HRP 1:10,000	GE Healthcare, Amersham, UK
Amyloid, precursor protein	Rabbit polyclonal 1:500	Abcam, Cambridge, MA, USA	Donkey anti-rabbit HRP 1:10,000	GE Healthcare, Amersham, UK
C-terminal, APP	Rabbit polyclonal 1:400	Millipore, Temecula, CA, USA	Donkey anti-rabbit, HRP 1:6,000	GE Healthcare, Amersham, UK
6E10	Mouse monoclonal 1:300	Covance, San Diego, CA, USA	Sheep anti-mouse, HRP 1:8,000	GE Healthcare, Amersham, UK
A11	Rabbit polyclonal 1:200	Invitrogen Camarillo, CA, USA	Donkey anti-rabbit, HRP 1:6,000	GE Healthcare, Amersham, UK
β-Actin	Mouse monoclonal 1:500	Sigma-Aldrich, St Louis, MO, USA	Sheep anti-mouse HRP 1:10,000	GE Healthcare, Amersham, UK

Briefly, protein cortical and hippocampal tissues from all four genotypes of mice were homogenized in a Tris-buffered saline (pH 8.0) containing protease inhibitors (20 mg/ml pepstatin A, aprotinin, phophsoramidon and leupeptin; 0.5 mM phenylmethanesulfonyl fluoride and 1 mM ethyleneglycol-bis(flaminoethyl ether)-NN tetraacetic acid). Samples were sonicated briefly and centrifuged at 10 000g for 20 min at 4°C. The soluble fraction was used to determine the soluble Aβ by ELISA. For each sample, Aβ1-40 and Aβ1-42 were measured with commercial colorimetric ELISA kits (Biosource International, Camarillo, CA, USA) specific for each species. A 96-well plate reader was used, following the manufacturer's instructions. Each sample was run in duplicate. Protein concentrations of the homogenates were determined following the BSA method, and Aβ was expressed as pg Aβ/mg protein.

Immunohistological analyses of total Aβ and Aβ40- and Aβ-specific deposits in AβPP and MCAT/AβPP mice

To determine the effects of MCAT in Aβ deposits, we performed immunohistochemistry and immunofluorescence analyses using the 6E10 antibody that recognizes both Aβ40 and Aβ42 deposits and also using end-specific Aβ40 and Aβ42 antibodies in the 12- and 24-month-old AβPP and MCAT/AβPP mice. We fixed the fresh-frozen midbrain sections (covering the hippocampus and cortex) from the AβPP and MCAT/AβPP mice by dipping the sections into a 4% paraformaldehyde solution for 10 min at room temperature. The sections were incubated overnight at room temperature with the 6E10 antibody (dilution 1:200; Covance). The next day, the sections were incubated with the secondary antibody conjugated with HRP or a biotin-labeled secondary antibody for 1 h, and additional sections were incubated with tyramide-labeled or the streptavidin-conjugated fluorescent dye, Alexa 594 (red) (Molecular Probes). Photographs were taken with a fluorescence microscope.

To determine Aβ40- and Aβ42-specific deposits, sections were pretreated with 50% formic acid for 5 min before they were labeled with the end-specific antibody stain anti-Aβ40 (BA27 clone; Wako Pure Chemicals, Japan) and anti-Aβ42 (AB05 clone, Wako Pure Chemicals). The sections were immunostained with BA27 and AB05 antibodies, using the same procedure that was used for the 6E10 antibody, except that the BA27 and AB05 antibody solutions were used without any dilution (according to the Wako kit manufacturer's instructions). Details of the antibodies are given in Table 6.

We quantified Aβ40- and Aβ42-specific deposits. In this quantification, we first viewed the sections that were immunostained with BA27 and AB05, using a ×2.5 objective that allowed us to view the entire cortex and hippocampus in one field. We then captured digital images of the field, using a fluorescence microscope (Zeiss Axioskop [40 FL]). We also took higher objective images (×5, ×20 and ×40). We background-subtracted the digital images and then performed quantitative analysis, using NIH ImageJ.

Immunohistochemistry of catalase, BACE1 and 8-hydroxydeoxyguanosine

To determine the effect of aging and MCAT on catalase, BACE1 and DNA damage, using the brain sections from

Table 6. Summary of antibody dilutions and conditions used in the immunohistochemistry/immunofluorescence using brain sections from transgenic mice and control WT mice

Marker	Primary antibody Species and dilution	Purchased from	Secondary antibody Dilution, Alexa dye	Purchased from
Anti-Aβ (6E10)	Mouse monoclonal 1:200	Covance, San Diego, CA, USA	Goat anti-mouse biotin 1:400, ABC, TSA-Alexa594	KPL, Gaithersburg, MD, USA VECTOR Laboratories, Burlingame, CA, USA Molecular Probes, Eugene, OR, USA
Anti-Aβ42 (AB05)	Mouse monoclonal (ready to use from the kit)	Wako Pure Chemicals, Japan	Goat anti-mouse biotin, ABC solution, TSA-Alexa594	Wako Pure Chemicals, Japan
Anti-Aβ40 (BA27)	Mouse monoclonal (ready to use from the kit)	Wako Pure Chemicals, Japan	Goat anti-mouse biotin, ABC solution, TSA-Alexa594	Wako Pure Chemicals, Japan
Catalase	Rabbit polyclonal 1:200	Abcam, Cambridge, MA, USA	Goat anti-rabbit biotin 1:400, ABC, TSA-Alexa 488	KPL, Gaithersburg, MD, USA VECTOR Laboratories, Burlingame, CA, USA Molecular Probes, Eugene, OR, USA
BACE1	Rabbit polyclonal 1:150	Calbiochem, San Diego, CA, USA	Goat anti-rabbit biotin 1:400, ABC,TSA-Alexa488	KPL, Gaithersburg, MD, USA VECTOR Laboratories, Burlingame, CA, USA Molecular Probes, Eugene, OR, USA
8-OHdG	Goat polyclonal, 1:200	Neuromics, Edina, MN, USA	Horse anti-goat biotin, 1:400, ABC,TSA-Alexa488	KPL, Gaithersburg, MD, USA VECTOR Laboratories, Burlingame, CA, USA Molecular Probes, Eugene, OR, USA

12- and 24-month-old MCAT, AβPP, MCAT/AβPP and WT mice, we also conducted immunostaining analyses, as described previously (61). Briefly, we fixed the fresh-frozen midbrain sections (covering the hippocampus and cortex) from the mice by dipping the sections into a 4% paraformaldehyde solution for 10 min at room temperature. The sections were then incubated with primary antibodies catalase (dilution, 1:200 rabbit polyclonal; Abcam), BACE1 (dilution, 1:150, rabbit polyclonal; Calbiochem) and 8-OHdG (dilution, 1:200, goat polyclonal; Neuromics, Edina, MN, USA) overnight at room temperature (Table 6.) The next day, the sections were incubated with an appropriate secondary antibody conjugated with HRP or a biotin-labeled secondary antibody for 1 h, and further sections were incubated with tyramide-labeled or streptavidin-conjugated fluorescent dye, Alexa 488 (green) (Molecular Probes). Photographs were taken using a fluorescence microscope. Randomly selected immunofluorescence images from cerebral cortex sections at ×40 magnification were analyzed with ImageJ to determine the relative immunofluorescence intensity for catalase, BACE1 and 8-OHdG in the 12- and 24-month-old MCAT, AβPP, MCAT/AβPP and WT mice. We compared the data between the mutant and WT mice.

BACE1 activity assay

BACE1 enzyme activity was measured in cortical protein lysates prepared from the 6-, 12- and 24-month-old MCAT, AβPP, MCAT/AβPP and WT mice, using a 96-well SensiZyme BACE1 Activity Assay Kit (Sigma-Aldrich, St Louis, MO, USA) based on the manufacturer's instructions, with minor modifications. BACE was measured using protein lysates from cortical tissues from all four genotypes of mice using the SensiZyme Assay Kit. The BACE1 standard or brain sample was applied into a well coated with a BACE1-specific antibody. A modified protein substrate (Substrate A) was added to the well. This antibody is a proenzyme containing the BACE1 protease-specific cleavage site fused to another protease. The proenzyme substrate was cleaved by BACE1 to form an active, 'new' protease. A colorimetric peptide substrate for this protease (Substrate B) was added to the well, which the protease cleaves. BACE1 activity was directly proportional to the generation of color. The change in the absorption of the chromogenic product was measured with a plate reader (Bio-Teck, Taunton, MA, USA) at an optical density of 405 nm. Brain tissues were homogenized and lysed in a lysis buffer (RIPA buffer; Thermo, Rockford, IL, USA) with a protease inhibitor cocktail (Sigma-Aldrich). For each measurement, 40 μg of total tissue extract was tested after an overnight incubation (more than 7 h) instead of just a few hours (e.g. 3–5 h). Five to eight samples in each group of extracts were used. Results were expressed as OD450 (mean ± SEM).

Behavioral test

Nose-poke tests were administered, following Tucci *et al*. and Moy *et al.* (33). Recently, the nose-poke test is thought to be a useful high-throughput method for the cognitive testing of rodents (32–35). The nose-poke test was assessed by 10-min trials (1 per day) in an open field chamber (27 × 27 × 20.3 cm), following the instructions (MED Associates, Inc., Vermont, USA). A floorboard with 16 equidistant holes was placed on the bottom of the chamber, with an infrared (I/R)

transmitter and receiver system (MED Associates, Inc.). Wire-mesh screens were placed 15 mm underneath each hole. The screens were used to prevent mice from touching objects placed in the holes during the subsequent tests with olfactory stimuli. The total distance the mouse traveled during each test was also recorded. Floorboards were removed after each test, washed with soapy water, wiped clean with paper towels and dried before the next mouse was tested.

Twelve-month-old MCAT ($n = 10$), AβPP ($n = 10$), MCAT/AβPP ($n = 6$) and WT ($n = 10$) were tested at light time period or their general exploratory behavior. Before we tested the mice, we trained them. We placed the food in two central holes and two wall holes. All animals (without food deprivation) were trained for three trials on each day. This training allowed the mice to acclimate to handling, to the environment and also to learn which holes had the food. Within 1 week of training, the nose-poke tests were performed and repeated in different days. All mice were food-deprived overnight before the test. The mice were observed for some time every day, while they went around the chamber, poking their noses into the holes, presumably looking for food. Only the food-baited holes that the mouse poked his/her nose into were used as contributing to the total nose-poke count aimed at the food target. This count was taken to represent the mouse's olfactory function and memory, i.e. increased such number of nose pokes indicates increased memory and learning. Data were expressed as the mean ± SEM.

Data analysis

Data were expressed as the mean ± SEM, except where otherwise indicated. Statistical comparisons were made, using ANOVA and Student's *t*-test with SigmaStat 3.5 software; $P < 0.05$ was considered statistically significant. Lifespan data were plotted using the Kaplan–Meier survival curves and were compared pairwise using a logrank test with primer 3 software. Median lifespan and maximum lifespan were calculated for each group.

SUPPLEMENTARY MATERIAL

Supplementary Material is available at *HMG* online.

ACKNOWLEDGEMENTS

We thank Dr Anda Cornea (Imaging Core of the OHSU Oregon National Primate Research Center) for her assistance with the confocal microscopy. We thank Dr Jodi L. McBride and Brett Dufour for their assistance with cognitive behavioral assessment. We also thank Dr Lauren Drew Martin, Veterinarian and animal facility staff, Katherine Marshall, Lorna Chandler, Haley Wolford, Melissa Holmes and William Worth, who diligently cared for all of the mice used in this study.

Conflict of Interest statement. None declared.

FUNDING

This research was supported by NIH grants AG028072, AG026051, RR000163 (P.H.R.) and P30-NS061800 (PI, Aicher) and a grant from the Alzheimer Association (IIRG-09-92429 to P.H.R.).

REFERENCES

1. Querfurth, H.W. and LaFerla, F.M. (2010) Alzheimer's disease. *N. Engl. J. Med.*, **362**, 329–344.
2. Mattson, M.P. (2004) Pathways towards and away from Alzheimer's disease. *Nature*, **430**, 631–639.
3. Reddy, P.H. and Beal, M.F. (2008) Amyloid beta, mitochondrial dysfunction and synaptic damage: implications for cognitive decline in aging and Alzheimer's disease. *Trends Mol. Med.*, **14**, 45–53.
4. Swerdlow, R.H. (2011) Brain aging, Alzheimer's disease, and mitochondria. *Biochim. Biophys. Acta*, **1812**, 1630–1639.
5. Mao, P. and Reddy, P.H. (2011) Aging and amyloid beta-induced oxidative DNA damage and mitochondrial dysfunction in Alzheimer's disease: implications for early intervention and therapeutics. *Biochim. Biophys. Acta*, **1812**, 1359–1370.
6. Reddy, P.H. (2006) Amyloid precursor protein-mediated free radicals and oxidative damage: implications for the development and progression of Alzheimer's disease. *J. Neurochem.*, **96**, 1–13.
7. Shen, C., Chen, Y., Liu, H., Zhang, K., Zhang, T., Lin, A. and Jing, N. (2008) Hydrogen peroxide promotes Abeta production through JNK-dependent activation of gamma-secretase. *J. Biol. Chem.*, **283**, 17721–17730.
8. Tamagno, E., Guglielmotto, M., Aragno, M., Borghi, R., Autelli, R., Giliberto, L., Muraca, G., Danni, O., Zhu, X., Smith, M.A. *et al.* (2008) Oxidative stress activates a positive feedback between the gamma- and beta-secretase cleavages of the beta-amyloid precursor protein. *J. Neurochem.*, **104**, 683–695.
9. Leuner, K., Schütt, T., Kurz, C., Eckert, S.H., Schiller, C., Occhipinti, A., Mai, S., Jendrach, M., Eckert, G.P., Kruse, S.E. *et al.* (2012) Mitochondria-derived ROS lead to enhanced amyloid beta formation. *Antioxid. Redox Signal.*, 2012 [Epub ahead of print].
10. Nunomura, A., Perry, G., Aliev, G., Hirai, K., Takeda, A., Balraj, E.K., Jones, P.K., Ghanbari, H., Wataya, T., Shimohama, S. *et al.* (2001) Oxidative damage is the earliest event in Alzheimer disease. *J. Neuropathol. Exp. Neurol.*, **60**, 759–767.
11. Praticò, D., Uryu, K., Leight, S., Trojanoswki, J.Q. and Lee, V.M. (2001) Increased lipid peroxidation precedes amyloid plaque formation in an animal model of Alzheimer amyloidosis. *J. Neurosci.*, **21**, 4183–4187.
12. Reddy, P.H. (2007) Mitochondrial dysfunction in aging and Alzheimer's disease: strategies to protect neurons. *Antioxid. Redox Signal.*, **9**, 1647–1658.
13. Manczak, M., Park, B.S., Jung, Y. and Reddy, P.H. (2004) Differential expression of oxidative phosphorylation genes in patients with Alzheimer's disease: implications for early mitochondrial dysfunction and oxidative damage. *Neuromol. Med.*, **5**, 147–162.
14. Devi, L., Prabhu, B.M., Galati, D.F., Avadhani, N.G. and Anandatheerthavarada, H.K. (2006) Accumulation of amyloid precursor protein in the mitochondrial import channels of human Alzheimer's disease brain is associated with mitochondrial dysfunction. *J. Neurosci.*, **26**, 9057–9068.
15. Caspersen, C., Wang, N., Yao, J., Sosunov, A., Chen, X., Lustbader, J.W., Xu, H.W., Stern, D., McKhann, G. and Yan, S.D. (2005) Mitochondrial abeta: a potential focal point for neuronal metabolic dysfunction in Alzheimer's disease. *FASEB J.*, **19**, 2040–2041.
16. Wang, X., Su, B., Siedlak, S.L., Moreira, P.I., Fujioka, H., Wang, Y., Casadesus, G. and Zhu, X. (2008) Amyloid-beta overproduction causes abnormal mitochondrial dynamics via differential modulation of mitochondrial fission/fusion proteins. *Proc. Natl Acad. Sci. USA*, **105**, 19318–19323.
17. Wang, X., Su, B., Lee, H.G., Li, X., Perry, G., Smith, M.A. and Zhu, X. (2009) Impaired balance of mitochondrial fission and fusion in Alzheimer's disease. *J. Neurosci.*, **29**, 9090–9103.
18. Aleardi, A.M., Benard, G., Augereau, O., Malgat, M., Talbot, J.C., Mazat, J.P, Letellier, T., Dachary-Prigent, J., Solaini, G.C. and Rossignol, R. (2005) Gradual alteration of mitochondrial structure and function by

beta-amyloids: importance of membrane viscosity changes, energy deprivation, reactive oxygen species production, and cytochrome c release. *J. Bioenerg. Biomembr.*, **37**, 207–225.
19. Manczak, M., Anekonda, T.S., Henson, E., Park, B.S., Quinn, J. and Reddy, P.H. (2006) Mitochondria are a direct site of A beta accumulation in Alzheimer's disease neurons: implications for free radical generation and oxidative damage in disease progression. *Hum. Mol. Genet.*, **15**, 1437–1449.
20. Manczak, M., Mao, P., Calkins, M.J., Cornea, A., Reddy, A.P., Murphy, M.P., Szeto, H.H., Park, B. and Reddy, P.H. (2010) Mitochondria-targeted antioxidants protect against amyloid-beta toxicity in Alzheimer's disease neurons. *J. Alzheimers Dis.*, **20**, S609–S631.
21. Calkins, M.J., Manczak, M., Mao, P., Shirendeb, U. and Reddy, P.H. (2011) Impaired mitochondrial biogenesis, defective axonal transport of mitochondria, abnormal mitochondrial dynamics and synaptic degeneration in a mouse model of Alzheimer's disease. *Hum. Mol. Genet.*, **20**, 4515–4529.
22. Yao, J., Irwin, R.W., Zhao, L., Nilsen, J., Hamilton, R.T. and Brinton, R.D. (2009) Mitochondrial bioenergetic deficit precedes Alzheimer's pathology in female mouse model of Alzheimer's disease. *Proc. Natl Acad. Sci. USA*, **106**, 14670–14675.
23. Rhein, V., Song, X., Wiesner, A., Ittner, L.M., Baysang, G., Meier, F., Ozmen, L., Bluethmann, H., Dröse, S., Brandt, U. *et al.* (2009) Amyloid-beta and tau synergistically impair the oxidative phosphorylation system in triple transgenic Alzheimer's disease mice. *Proc. Natl Acad. Sci. USA*, **106**, 20057–20062.
24. Du, H., Guo, L., Yan, S., Sosunov, A.A., McKhann, G.M. and Yan, S.S. (2010) Early deficits in synaptic mitochondria in an Alzheimer's disease mouse model. *Proc. Natl Acad. Sci. USA*, **107**, 18670–18675.
25. Devi, L. and Ohno, M. (2012) Mitochondrial dysfunction and accumulation of the β-secretase-cleaved C-terminal fragment of APP in Alzheimer's disease transgenic mice. *Neurobiol. Dis.*, **45**, 417–424.
26. Manczak, M., Calkins, M.J. and Reddy, P.H. (2011) Impaired mitochondrial dynamics and abnormal interaction of amyloid beta with mitochondrial protein Drp1 in neurons from patients with Alzheimer's disease: implications for neuronal damage. *Hum. Mol. Genet.*, **20**, 2495–2509.
27. Crouch, P.J., Blake, R., Duce, J.A., Ciccotosto, G.D., Li, Q.X., Barnham, K.J., Curtain, C.C., Cherny, R.A., Cappai, R., Dyrks, T., Masters, C.L. and Trounce, I.A. (2005) Copper-dependent inhibition of human cytochrome c oxidase by a dimeric conformer of amyloid-beta1–42. *J. Neurosci.*, **25**, 672–679.
28. Du, H., Guo, L., Fang, F., Chen, D., Sosunov, A.A., McKhann, G.M., Yan, Y., Wang, C., Zhang, H., Molkentin, J.D. *et al.* (2008) Cyclophilin D deficiency attenuates mitochondrial and neuronal perturbation and ameliorates learning and memory in Alzheimer's disease. *Nat. Med.*, **14**, 1097–1105.
29. Hansson Petersen, C.A., Alikhani, N., Behbahani, H., Wiehager, B., Pavlov, P.F., Alafuzoff, I., Leinonen, V., Ito, A., Winblad, B., Glaser, E. and Ankarcrona, M. (2009) The amyloid beta-peptide is imported into mitochondria via the TOM import machinery and localized to mitochondrial cristae. *Proc. Natl Acad. Sci. USA*, **105**, 13145–13150.
30. Schriner, S.E., Linford, N.J., Martin, G.M., Treuting, P., Ogburn, C.E., Emond, M., Coskun, P.E., Ladiges, W., Wolf, N., Van Remmen, H., Wallace, D.C. and Rabinovitch, P.S. (2005) Extension of murine life span by overexpression of catalase targeted to mitochondria. *Science*, **308**, 1909–1911.
31. Hsiao, K., Chapman, P., Nilsen, S., Eckman, C., Harigaya, Y., Younkin, S., Yang, F. and Cole, G. (1996) Correlative memory deficits, Abeta elevation, and amyloid plaques in transgenic mice. *Science*, **274**, 99–102.
32. Tucci, V., Hardy, A. and Nolan, P.M. (2006) A comparison of physiological and behavioural parameters in C57BL/6J mice undergoing food or water restriction regimes. *Behav. Brain Res.*, **173**, 22–29.
33. Moy, S.S., Nadler, J.J., Poe, M.D., Nonneman, R.J., Young, N.B., Koller, B.H., Crawley, J.N., Duncan, G.E. and Bodfish, J.W. (2008) Development of a mouse test for repetitive, restricted behaviors: relevance to autism. *Behav. Brain Res.*, **188**, 178–194.
34. Krueger, D.D., Osterweil, E.K., Chen, S.P., Tye, L.D. and Bear, M.F. (2011) Cognitive dysfunction and prefrontal synaptic abnormalities in a mouse model of fragile X syndrome. *Proc. Natl Acad. Sci. USA*, **108**, 2587–2592.
35. Bussey, T.J., Holmes, A., Lyon, L., Mar, A.C., McAllister, K.A., Nithianantharajah, J., Oomen, C.A. and Saksida, L.M. (2012) New translational assays for preclinical modelling of cognition in schizophrenia: the touchscreen testing method for mice and rats. *Neuropharmacology*, **62**, 1191–1203.
36. Lagadec, S., Rotureau, L., Hémar, A., Macrez, N., Delcasso, S., Jeantet, Y. and Cho, Y.H. (2012) Early temporal short-term memory deficits in double transgenic APP/PS1 mice. *Neurobiol. Aging*, **33**, 203.e1–203.e11.
37. Mumby, D.G., Gaskin, S., Glenn, M.J., Schramek, T.E. and Lehmann, H. (2002) Hippocampal damage and exploratory preferences in rats: memory for objects, places, and contexts. *Learn. Mem.*, **9**, 49–57.
38. Bacon, A.W., Bondi, M.W., Salmon, D.P. and Murphy, C. (1998) Very early changes in olfactory functioning due to Alzheimer's disease and the role of apolipoprotein E in olfaction. *Ann. N Y Acad. Sci.*, **855**, 723–731.
39. Kovacs, T. (2004) Mechanisms of olfactory dysfunction in aging and neurodegenerative disorders. *Ageing Res. Rev.*, **3**, 215–232.
40. Roberds, S.L., Anderson, J., Basi, G., Bienkowski, M.J., Branstetter, D.G., Chen, K.S., Freedman, S.B., Frigon, N.L., Games, D., Hu, K. *et al.* (2001) BACE knockout mice are healthy despite lacking the primary beta-secretase activity in brain: implications for Alzheimer's disease therapeutics. *Hum. Mol. Genet.*, **10**, 1317–1324.
41. Vassar, R., Kovacs, D.M., Yan, R. and Wong, P.C. (2009) The beta-secretase enzyme BACE in health and Alzheimer's disease: regulation, cell biology, function, and therapeutic potential. *J. Neurosci.*, **29**, 12787–12794.
42. Ohn, M., Chang, L., Tseng, W., Oakley, H., Citron, M., Klein, W.L., Vassar, R. and Disterhoft, J.F. (2006) Temporal memory deficits in Alzheimer's mouse models: rescue by genetic deletion of BACE1. *Eur. J. Neurosci.*, **23**, 251–260.
43. Tamagno, E., Bardini, P., Obbili, A., Vitali, A., Borghi, R., Zaccheo, D., Pronzato, M.A., Danni, O., Smith, M.A., Perry, G. and Tabaton, M. (2002) Oxidative stress increases expression and activity of BACE in NT2 neurons. *Neurobiol. Dis.*, **10**, 279–288.
44. Wen, Y., Onyewuchi, O., Yang, S., Liu, R. and Simpkins, J.W. (2004) Increased beta-secretase activity and expression in rats following transient cerebral ischemia. *Brain Res.*, **1009**, 1–8.
45. Zhang, X., Zhou, K., Wang, R., Cui, J., Lipton, S.A., Liao, F.F., Xu, H. and Zhang, Y.W. (2007) Hypoxia-inducible factor 1alpha (HIF-1alpha)-mediated hypoxia increases BACE1 expression and beta-amyloid generation. *J. Biol. Chem.*, **282**, 10873–10880.
46. Guglielmotto, M., Aragno, M., Autelli, R., Giliberto, L., Novo, E., Colombatto, S., Danni, O., Parola, M., Smith, M.A., Perry, G., Tamagno, E. and Tabaton, M. (2009) The up-regulation of BACE1 mediated by hypoxia and ischemic injury: role of oxidative stress and HIF1alpha. *J. Neurochem.*, **108**, 1045–1056.
47. Huang, X., Cuajungco, M.P., Atwood, C.S., Hartshorn, M.A., Tyndall, J.D., Hanson, G.R., Stokes, K.C., Leopold, M., Multhaup, G., Goldstein, L.E. *et al.* (1999) Cu(II) potentiation of Alzheimer abeta neurotoxicity. Correlation with cell-free hydrogen peroxide production and metal reduction. *J. Biol. Chem.*, **274**, 37111–37116.
48. Tabner, B.J., El-Agnaf, O.M., Turnbull, S., German, M.J., Paleologou, K.E., Hayashi, Y., Cooper, L.J., Fullwood, N.J. and Allsop, D. (2205) Hydrogen peroxide is generated during the very early stages of aggregation of the amyloid peptides implicated in Alzheimer disease and familial British dementia. *J. Biol. Chem.*, **280**, 35789–35792.
49. De Felice, F.G., Velasco, P.T., Lambert, M.P., Viola, K., Fernandez, S.J., Ferreira, S.T. and Klein, W.L. (2007) Abeta oligomers induce neuronal oxidative stress through an N-methyl-D-aspartate receptor-dependent mechanism that is blocked by the Alzheimer drug memantine. *J. Biol. Chem.*, **282**, 11590–11601.
50. Behl, C., Davis, J.B., Lesley, R. and Schubert, D. (1994) Hydrogen peroxide mediates amyloid beta protein toxicity. *Cell*, **77**, 817–827.
51. Sagara, Y., Tan, S., Maher, P. and Schubert, D. (1998) Mechanisms of resistance to oxidative stress in Alzheimer's disease. *Biofactors*, **8**, 45–50.
52. Dai, D.F., Santana, L.F., Vermulst, M., Tomazela, D.M., Emond, M.J., MacCoss, M.J., Gollahon, K., Martin, G.M., Loeb, L.A., Ladiges, W.C. and Rabinovitch, P.S. (2009) Overexpression of catalase targeted to mitochondria attenuates murine cardiac aging. *Circulation*, **119**, 2789–2797.
53. Dai, D.F., Chen, T., Wanagat, J., Laflamme, M., Marcinek, D.J., Emond, M.J., Ngo, C.P., Prolla, T.A. and Rabinovitch, P.S. (2010) Age-dependent

cardiomyopathy in mitochondrial mutator mice is attenuated by overexpression of catalase targeted to mitochondria. *Aging Cell*, **9**, 536–544.
54. Lee, H.Y., Choi, C.S., Birkenfeld, A.L., Alves, T.C., Jornayvaz, F.R., Jurczak, M.J., Zhang, D., Woo, D.K., Shadel, G.S., Ladiges, W. *et al.* (2010) Targeted expression of catalase to mitochondria prevents age-associated reductions in mitochondrial function and insulin resistance. *Cell Metab*., **12**, 668–674.
55. Treuting, P.M., Linford, N.J., Knoblaugh, S.E., Emond, M.J., Morton, J.F., Martin, G.M., Rabinovitch, P.S. and Ladiges, W.C. (2008) Reduction of age-associated pathology in old mice by overexpression of catalase in mitochondria. *J. Gerontol. A Biol. Sci. Med. Sci.*, **63**, 813–822.
56. Mecocci, P., MacGarvey, U. and Beal, M.F. (1994) Oxidative damage to mitochondrial DNA is increased in Alzheimer's disease. *Ann. Neurol.*, **36**, 747–751.
57. Lyras, L., Cairns, N.J., Jenner, A., Jenner, P. and Halliwell, B. (1997) An assessment of oxidative damage to proteins, lipids, and DNA in brain from patients with Alzheimer's disease. *J. Neurochem.*, **68**, 2061–2069.
58. Gabbita, S.P., Lovell, M.A. and Markesbery, W.R. (1998) Increased nuclear DNA oxidation in the brain in Alzheimer's disease. *J. Neurochem.*, **71**, 2034–2040.
59. Wang, J., Xiong, S., Xie, C., Markesbery, W.R. and Lovell, M.A. (2005) Increased oxidative damage in nuclear and mitochondrial DNA in Alzheimer's disease. *J. Neurochem.*, **93**, 953–962.
60. Wang, J., Markesbery, W.R. and Lovell, M.A. (2006) Increased oxidative damage in nuclear and mitochondrial DNA in mild cognitive impairment. *J. Neurochem.*, **96**, 825–832.
61. Manczak, M., Mao, P., Nakamura, K., Bebbington, C., Park, B. and Reddy, P.H. (2009) Neutralization of granulocyte macrophage colony-stimulating factor decreases amyloid beta 1-42 and suppresses microglial activity in a transgenic mouse model of Alzheimer's disease. *Hum. Mol. Genet.*, **18**, 3876–3893.
62. Shirendeb, U., Reddy, A.P., Manczak, M., Calkins, M.J., Mao, P., Tagle, D.A. and Reddy, P.H. (2011) Abnormal mitochondrial dynamics, mitochondrial loss and mutant huntingtin oligomers in Huntington's disease: implications for selective neuronal damage. *Hum. Mol. Genet.*, **20**, 1438–1455.
63. Laws, G.M. and Adams, S.P. (1996) Measurement of 8-OHdG in DNA by HPLC/ECD: the importance of DNA purity. *BioTechniques*, **20**, 36–38.
64. Lau, S.S., Peters, M.M., Kleiner, H.E., Canales, P.L. and Monks, T.J. (1996) Linking the metabolism of hydroquinone to its nephrotoxicity and nephrocarcinogenicity. *Adv. Exp. Med. Biol.*, **387**, 267–273.